2020

# Thermal analysis and designs for non-radioactive thermoelectric generators for common small satellite types

BOSTON UNIVERSITY

COLLEGE OF ENGINEERING

Thesis

# THERMAL ANALYSIS AND DESIGNS FOR NON-RADIOACTIVE THERMOELECTRIC GENERATORS FOR COMMON SMALL SATELLITE TYPES

by

**DAVID ARTHUR PAYNE**

B.A., Rice University, 2013
M.P.P., Harvard University, 2017

Submitted in partial fulfillment of the

requirements for the degree of

Master of Science

2020

Approved by

First Reader

Joshua L. Semeter, Ph.D.
Professor of Electrical and Computer Engineering

Second Reader

Brian M. Walsh, Ph.D.
Assistant Professor of Mechanical Engineering
Assistant Professor of Electrical and Computer Engineering

Third Reader

J. William Boley, Ph.D.
Assistant Professor of Mechanical Engineering
Assistant Professor of Materials Science and Engineering

## ACKNOWLEDGMENTS

This thesis would not be possible without the help, guidance, and support of others. First off is my advisor, Professor Brian Walsh, who provided the original impetus for this project and supported it throughout offering guidance and help. Other members of the Space Physics and Technology Lab, specifically Emil Atz and Aleks Zosuls, provided invaluable help with using lab equipment for design as well as testing and Aily Walker helped with initial background research.

This project was greatly improved by the guidance and support of Professors Josh Semeter and Will Boley who generously offered their time to serve on the committee.

A key part of this project was to determine the thermal energy available on small satellites. While this project was originally scoped to only rely upon thermal models, it was greatly improved by the generosity of Spire and of Lawrence Kepko from NASA Goddard Space Flight Center in providing on-orbit thermal data. To support the thermal modeling, Cullimore and Ring Technologies generously provided use of their industry-standard Thermal Desktop software for use in this project.

This thesis would not have been possible without all the help from those listed above as well as numerous others who provided assistance, advice, input, support, and thoughts throughout the process. For all of that, I am very grateful.

**THERMAL ANALYSIS AND DESIGNS FOR**

**NON-RADIOACTIVE THERMOELECTRIC GENERATORS**

**FOR COMMON SMALL SATELLITE TYPES**

**DAVID ARTHUR PAYNE**

ABSTRACT

Small satellites on-orbit generate power today via solar panels. As more power-hungry parts are incorporated and the room to grow solar panel coverage is limited, power budgets are increasingly strained. Thermoelectric generators, which produce power from thermal gradients, present a possible secondary power source to help relax those constraints. Satellites on-orbit can see large temperature gradients, upwards of 100 degrees Celsius, due to their environment. These large gradients are well-suited for thermoelectrics to harvest. This project characterized the opportunity for such generators via thermal modeling and analysis of on-orbit thermal data and used solar panel data for performance comparison. Specific power for solar panels, calculated from information on published datasheets, ranged from 20.15 to 53.7 W/kg and hypothetical thermoelectric generators in this project harvesting thermal energy showed specific powers ranging from 10.25 to 154.99 W/kg. Based on the results, there is an opportunity for thermoelectrics competitive with solar panels and the greatest opportunity is on the back of deployed solar panels where the max specific power of 154.99 W/kg was found under certain parameters. This project used that data to drive the design of a planar thermoelectric generator as

might be placed on the back of a deployed panel. The concept of using two FR-4 printed-circuit boards with thermoelectric elements sandwiched in between was validated and next steps for a functioning prototype outlined. This project also began an exploration into different internal architectures of a thermoelectric generator beyond a traditional grid and while no actionable results were found, it is believed that this is an area worth future work. The key takeaway is that this project lends support to the idea of trialing a thermoelectric generator on a small satellite to harvest environmental heat differences on such satellites.

## TABLE OF CONTENTS

## LIST OF TABLES

## LIST OF FIGURES

## LIST OF ABBREVIATIONS

BCR ..... Battery Charge Regulator

BU ..... Boston University

CAD ..... Computer Aided Design

EM..... Electromagnetic Radiation

IR ..... Infrared

ISS ..... International Space Station

LEO..... Low-Earth Orbit

MCU..... Main Control Unit

N.D. ..... No Date

OBC ..... On-Board Computer

PCB..... Printed Circuit Board

PDU ..... Power Distribution Unit

SoC ..... System-On-Chip

SWaP..... Size, Weight, and Power

TCS..... Thermal Control System

TD ..... Thermal Desktop

TEG..... Thermoelectric Generator

# INTRODUCTION

Small satellite designers work within very tight power budgets that limit what can be done and what percent of the time the spacecraft can operate. At the present, low-Earth orbit (LEO) small satellites generate power by capturing solar energy in the form of photons.

Thermoelectrics present an alternative or supplemental form of power generation. A thermoelectric generator (TEG) converts the flow of thermal energy that comes from one side of the generator being hotter than the other to produce electric power. Some government spacecraft have used radioactive thermoelectric generators (Bennett, et al., 2006) but technical, cost, safety, and legal issues prevent radioactive sources from being adopted broadly.

The overall goal of this project was to (1) quantify the opportunity for a thermoelectric generator (TEG) on a low-Earth orbit (LEO) small satellite to generate power from environmental as opposed to radioactive-induced heat differences and (2) to design and build a prototype.

## Background on Small Satellites

Small satellites, commonly called “smallsats”, are an increasingly popular size of satellite and generally refers to satellites with a mass of 600 kg or less (Halt & Wieger, 2019). A common variant of this type of satellite is the “CubeSat” (See Appendix A for more information on CubeSats). Despite their diminutive size, they are being used and considered for more and more missions. From NASA’s recent use of them on a Mars mission (Jet Propulsion Laboratory, n.d.)

to Astranis's plan to use smallsats for geosynchronous orbit applications (Astranis, n.d.) to launch providers such as Rocket Lab planning standard launch offerings for such satellites beyond Earth orbit (O'Callaghan, 2019), their use cases are increasing.

The way small satellites generate power today is with solar panels. An example can be seen in Figure 1 with the satellite Dellingr. As can be seen in that figure, solar panels are placed on almost every external part of the satellite's chassis. If the designers had wanted to produce more power to support more power-intensive components or operational plans while retaining the same size chassis, their options are currently limited.

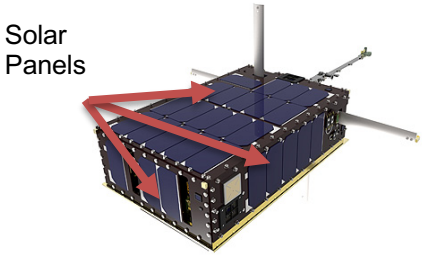


**Figure 1. Dellingr Small Satellite with Solar Panels Highlighted (NASA)**

One of those options is to deploy panels from the satellite and place solar cells on those panels. This approach can be seen in Figure 2 of a satellite from the company Spire.

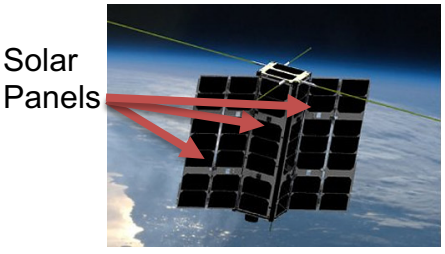


**Figure 2. Satellite with Solar Panels Highlighted (Spire)**

More complicated deployment mechanisms than what Spire used can be built to create even more available surface area for solar panels on-orbit. This project looks at a potentially lower-cost and lower-complexity way to generate power by taking advantage of temperature differentials.

## Background on Satellite Thermal Environment

Satellite manufacturers and operators care about the thermal environment because it affects the survivability and operability of various components. Generally, each component has two temperature ranges (See Figure 3 for an example):

- A “survival” temperature range that a component must stay within otherwise the component risks being permanently damaged or destroyed (e.g. melted)
- An “operating” temperature range that is equal to or narrower than the survival temperature range that a component must be within to function as desired. Given that when electronic systems are turned on, they generate heat, it is common that the system heats up after being turned on.[1] Therefore the low point of the operating temperature range is sometimes referred to as the ‘turn-on temperature’ or other similar term.

[1] This may not be true if heat is being conducted or emitted away from the component more quickly than the electronics are generating heat. For example, if a turned off cellphone is taken from room temperature, placed in a freezer, and then turned on, the effect of the freezer is likely to overwhelm the effect of the turned-on phone and therefore the phone will keep dropping in temperature.

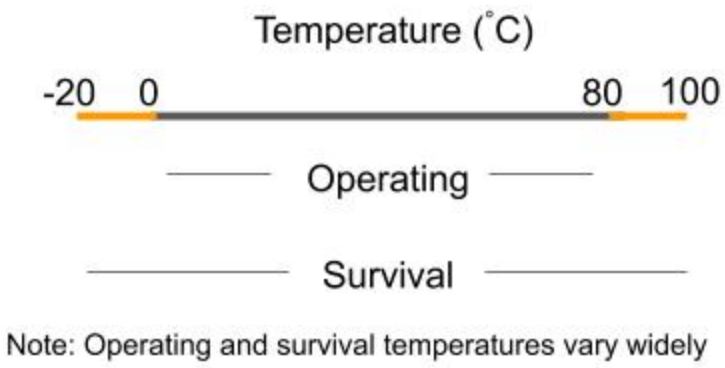


**Figure 3. Example of Operating and Survival Temperature Ranges**

A satellite in LEO has four sources of thermal energy: (1) radiation from the sun known as ‘solar flux’, (2) reflected radiation from the sun off the Earth commonly called ‘albedo’, (3) emitted radiation from the Earth due to its warmth commonly called ‘IR planetshine’, and (4) heat generated by the operations of the satellite itself. (See Figure 4 for a diagram of the four sources)

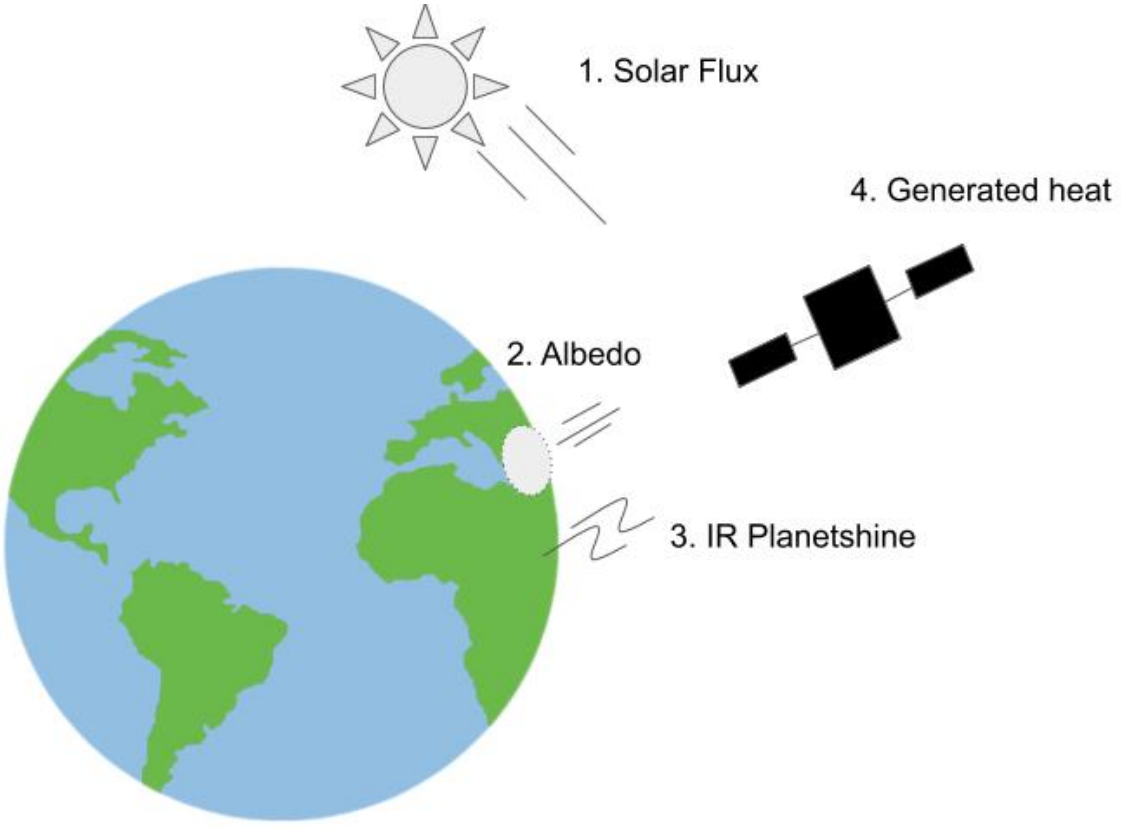


**Figure 4. Diagram of Sources of Thermal Energy for a LEO Satellite**[2]

These sources are not consistent over the life or obit of a satellite. There are a wide variety of reasons. A few examples: the albedo of materials varies and therefore the albedo off Earth is not consistent across the surface, the generated heat from a satellite will change as components are turned on or off at different points, and the amount of incident energy from each of the external sources will vary based on the orientation of the satellite. To highlight one particularly important factor – the solar flux will vary greatly with whether the satellite is within

[2] Generally, other sources of energy such as light from other stars, albedo off the moon and other heavenly bodies, heat from other artificial satellites, and conduction to the atmosphere are considered negligible. For satellites with especially sensitive components, these sources may have a meaningful impact or if a satellite is at an especially low orbit, atmospheric conduction may become meaningful.

view of the sun or is in an eclipse behind the Earth.

For every satellite, a defined thermal control system (TCS) should be developed. The overall goal of the TCS is to keep everything in survival range and to keep components in operating range when needed. For each component as well as for the satellite system, the heat-in vs. heat-out needs to be balanced to meet the goals of the mission.

The TCS can be made up of “passive” elements such as paints to increase or decrease reflectivity, “active” elements such as heaters, or a combination of the two. Some of these decisions, such as what paint to use, which components to incorporate, what component should go where, and whether to add heaters will be baked into the design with little to no ability to modify once the satellite is in orbit. Other decisions such as when and for how long to turn on various components and how to orient the satellite can generally be updated while in orbit.

The thermal environment on orbit can be extreme. For example, NASA has said that without any thermal controls, the International Space Station’s solar panels hot (sun-facing) sides would reach 121° C while the opposite cold sides would reach -157° C (NASA, 2001).

## Background on Thermoelectric Generators

### *Thermoelectric Operating Principles*

Thermoelectric Generators (TEG) work off the “Seebeck Effect” in reference to the man who figured out the principles of operation (Hunt, 1964).

They are solid-state (in other words, no moving parts). They have a mix of positively-doped (P-type) and negatively-doped (N-type) material blocks that are tiled onto a substrate. The heat gradient causes the movement of charge carriers across those materials. That movement causes a voltage to develop. See Figure 5 for a diagram and Figure 6 for an exploded computer-aided design (CAD) view of a TEG. The model shows the alternating P and N blocks denoting the positively doped and negatively doped semiconductor material sandwiched between two plates and connected out to the system via wires. The red sun indicates the hot side and the blue flake indicates the cold side.

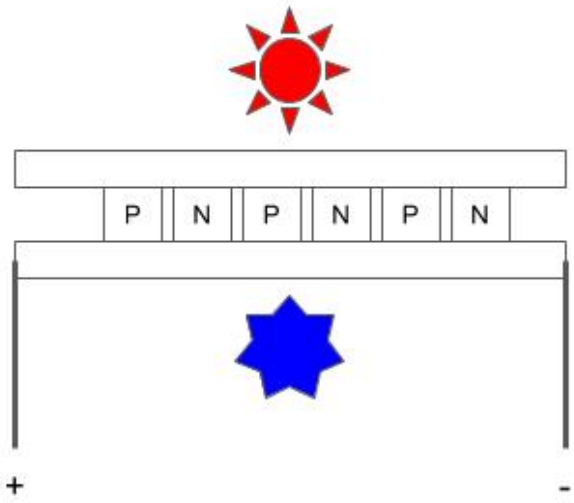


**Figure 5. Diagram of a Thermoelectric Generator**

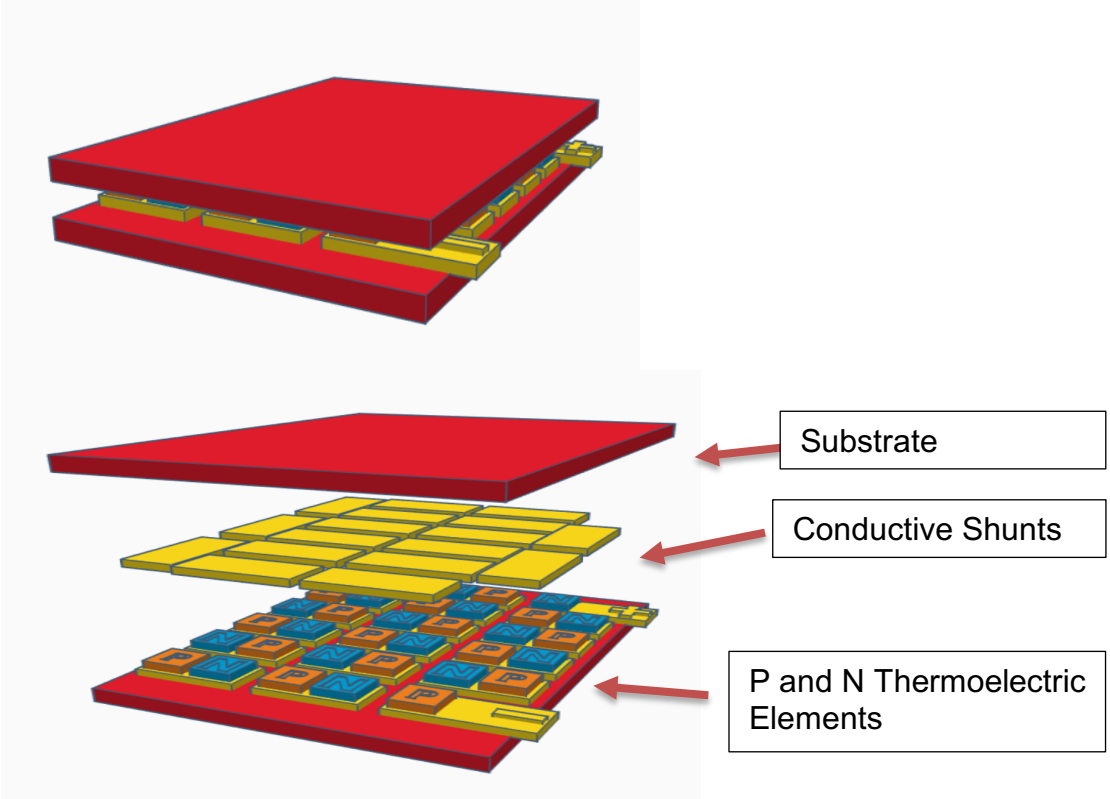


**Figure 6. Computer Design Model of a Thermoelectric Generator (TEG)**

On the top of Figure 6 is the assembled TEG and on the bottom is the exploded view of the TEG. The red is the electrically-insulating plates. The yellow is conductive material. The orange and blue are the positively and negatively, respectively, doped thermoelectric semiconductor material. Note: this TEG is laid out with a serial connection between the semiconductor blocks. This maximizes output voltage. It is possible to arrange the connections in parallel to maximize output current.

### *Thermoelectric Generator Use in Space*

Governmental agencies, e.g. the National Aeronautics and Space Administration (NASA), have used TEGs for their spacecraft before but they add in a radioactive source to provide a high and controllable heat source (Bennett, et al., 2006). This approach has been used on many NASA missions including the Cassini mission to Saturn and the New Horizons mission to Pluto. Both of those missions specifically used a device called the general-purpose heat source radioisotope thermoelectric generator (GPHS-RTG) that used plutonium as its energy source and a silicon-germanium (SiGe) alloy to create the thermoelectric elements (Bennett, et al., 2006).

NASA has developed other RTGs including the multi-mission radioisotope thermoelectric generator (MMRTG) that utilized lead-telluride and lead-tin-telluride to capture the power from the heat (Woerner, A Progress Report on the eMMRTG, 2016). And they designed an enhanced MMRTG called eMMRTG that utilized Skutterudite, a cobalt-arsenide, for the thermoelectric element (Woerner, A Progress Report on the eMMRTG, 2016). NASA also conducted a study on next-generation RTGs, identifying eight thermoelectric couples to continue study on (Matthes, et al., 2018). To note, unfortunately, that list and the larger report (Woerner, Next-Generation Radioisotope Thermoelectric Generator Study Final Report, 2017). cannot be leveraged for this project as it is export-controlled and restricted to current developers of RTGs for NASA.[3]

[3] Restrictions on use can be found in the report request form online (NASA, 2017)

Radioactive sources, while effective, are not practical for commercial satellites due to the cost[4], complexity, safety, and legal challenges that come with radioactive material.

The way that commercial satellites generate power today is via solar. This works well as solar energy is generally plentiful in space,[5] solar cells do not need moving parts, and it is a proven technology. The problem is that as satellites have gotten smaller, their hunger for power hasn't dropped nearly as much while the area available for solar panels decreases with the size. Companies have invested in increasingly efficient solar panels but gains at this point are minimal and are fundamentally limited in efficiency according to the Shockley-Queisser detailed balance model (Polman, Knight, Garnett, Ehrler, & Sinke, 2016).

There have been a couple of attempts to use non-radioactive TEGs in small spacecraft (Lukowicz, Abbe, Schmiel, & Tajmar, 2016), (Lappas, Tsourdos, Kindylides, & Kostopoulos, 2019). In these attempts, they have analyzed and shown the potential for non-radioactive TEGs use on a couple of specific small spacecraft models. They have found that there are large temperature differentials that could be harvested but there are a host of challenges. These challenges of using TEGs in space include the high rate of thermal cycling, vibrations during launch, the vacuum in space, surface area availability, and the low (5-7%) efficiency of TEGs (Lappas, Tsourdos, Kindylides, & Kostopoulos, 2019).

---

[4] For instance, the primary fuel source used in RTGs, Plutonium-238, costs $8 million a kilogram and the supply is very constrained (Oregon State University, n.d.)

[5] Solar energy decreases with distance from sun and there are some specialized orbits that see very minimal solar radiation such as the 2nd Lagrange Point (L2) (NASA, 2019)

A research team out of the United Kingdom and Greece tried to address the rapid thermal cycling challenge by introducing a microfluidics system to stabilize the temperature on each side of the TEG (Lappas, Tsourdos, Kindylides, & Kostopoulos, 2019). To highlight one issue with that approach, a fluidic system undercuts one of the central benefits of TEGs - the fact that they are solid-state and low complexity. While the authors claim the fluidic system wouldn't add complexity as it could take advantage of the same system used in some propulsion systems, many common small satellites, e.g. Planet's Doves (Zimmerman, et al., 2017) and Spire's Lemurs (Spire, 2015), do not use propulsion.

# CHAPTER ONE: THERMAL ANALYSIS AND MODELING

## Section One: Summary of Analysis and Modeling

The goal of this part of the project was (1) to determine the thermal energy available for a thermoelectric generator (TEG) on a low-Earth orbit (LEO) satellite and (2) to establish a baseline for performance to provide a comparison.

Solar panels are the predominant source of power for LEO satellites and published information on those panels was used to establish a baseline of performance. At the beginning of this project, the hypothesis was that the greatest temperature differentials, and therefore the biggest opportunity for TEGs would be on deployed components such as solar panels and dish antennas (See Figure 7) due to them having one side facing the sun and the other radiating to space without the moderating influence of the heat from a satellite's various processors and heaters inside the chassis.

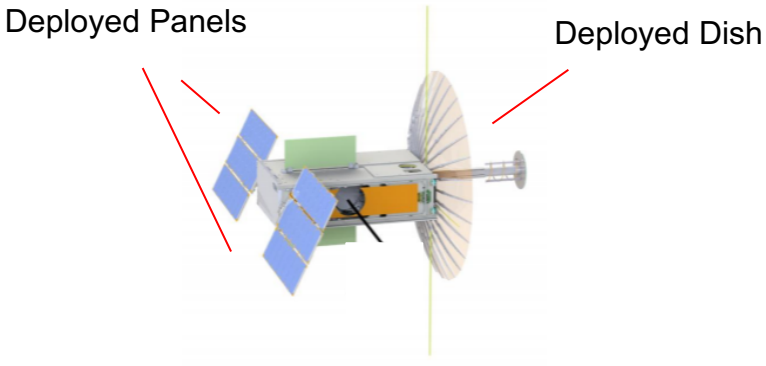


**Figure 7. Satellite with Deployed Solar Panels and Deployed Dish (Analytical Space, Inc., 2018)**

In summary, the results show that there is an operationally meaningful amount of thermal energy across the satellites analyzed due to the environment and dissipated power that a TEG could harness. Deployed panels had the highest temperature gradients. Additionally, the back of solar panels offers a flat surface which would allow for easy integration and the back of deployed panels are often not otherwise utilized. Due to these reasons, the back of deployed solar panels is the highest value candidate location. As with any model, there were a host of assumptions made. It is believed that while all individual assumptions would not hold in all cases, the top-line conclusion still holds and TEGs present an opportunity worth a trial on a LEO satellite.

On-orbit thermal data from four satellites, three from the company Spire and one from the National Aeronautics and Space Administration (NASA), was used as the main source of analysis for the availability and distribution of thermal energy. The NASA satellite does not have deployed panels and Spire did not have thermal data for the deployed panels on their satellites, so the on-orbit data was supplemented with thermal models conducted in the industry-standard software Thermal Desktop with the focus of those simulations being on deployables. Thermal Desktop allows for the setting of optical and thermophysical properties for different materials as well as orbital thermal flux parameters including solar, albedo, and IR planetshine (Parameters used can be found in Section Three).

As a first cut, satellite components are often evaluated by their size,

weight, and power (SWaP). All analysis was baselined to the size of a 1-unit (1U) panel of 10x10 centimeters, so the SWaP simplified to power provided per unit of mass, otherwise known as specific power, measured in watts per kilogram. Based upon looking at published data on five solar panels, a comparative baseline range of 20.15 to 53.7 W/kg was established.

Through analysis, the largest temperature differential found within the three Spire satellites was between the battery charge regulator (BCR) board and the system-on-chip (SoC) [See Figure 8 and Figure 9 for temperature profile for one satellite as an example]. Average temperature differences between those two points across the three satellites were 8.30, 9.21, and 16.28 degrees Celsius with a maximum temperature differential of 33.4°C. Two of those Spire satellites are in roughly 580-kilometer sun-synchronous orbits (SSO) and one is in an orbit similar to that of the International Space Station's, colloquially known as an "ISS orbit." The NASA satellite has solar panels mounted on its chassis with temperature sensors on both sides of several of those panels.

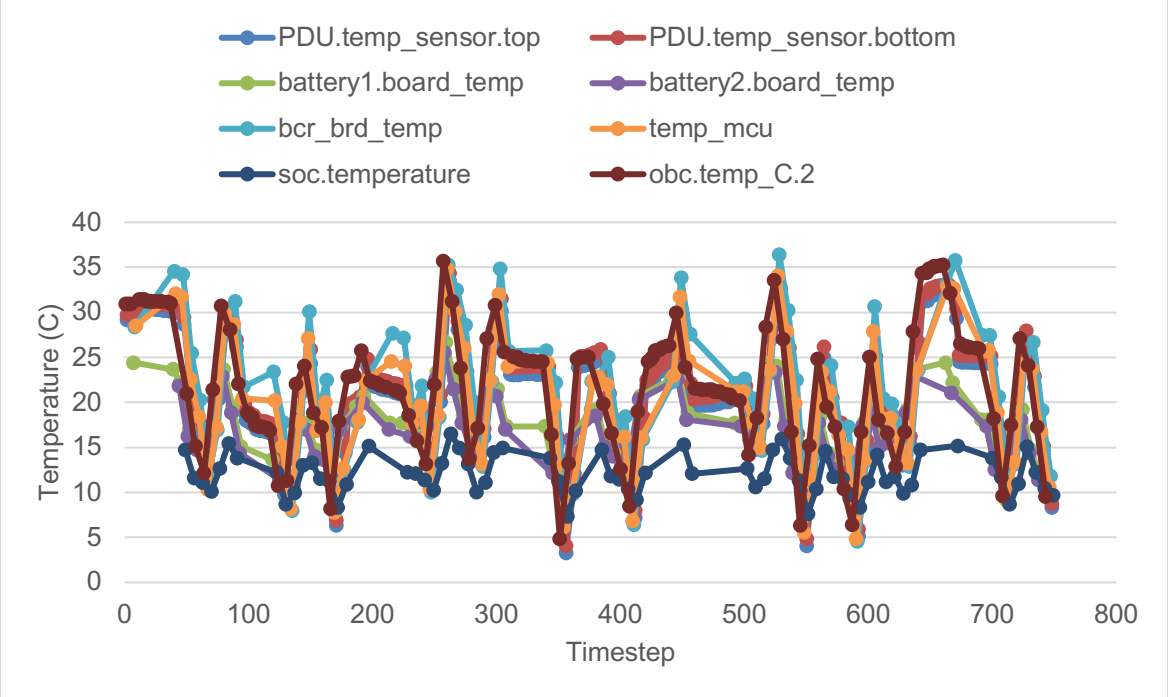


**Figure 8. SSO Satellite (FM79) Key Temperature Sensors[6,7]**

[6] Data are given over a 24-hour period. "Timestep" is used as timesteps between data points varied by sensor and over time. Straight-line data interpolation used to provide comparable data points. Further information on that methodology can be found in Section Three.

[7] Acronyms used are as provided in data file. Below is the believed correspondence.
BCR…Battery-Charge Regulator
MCU…Main Control Unit
OBC…On-Board Computer
PDU…Power-Distribution Unit
SoC…System-On-Chip
A CAD file was not provided with the data so the spatial distribution, use profile, and other characteristics are not known.

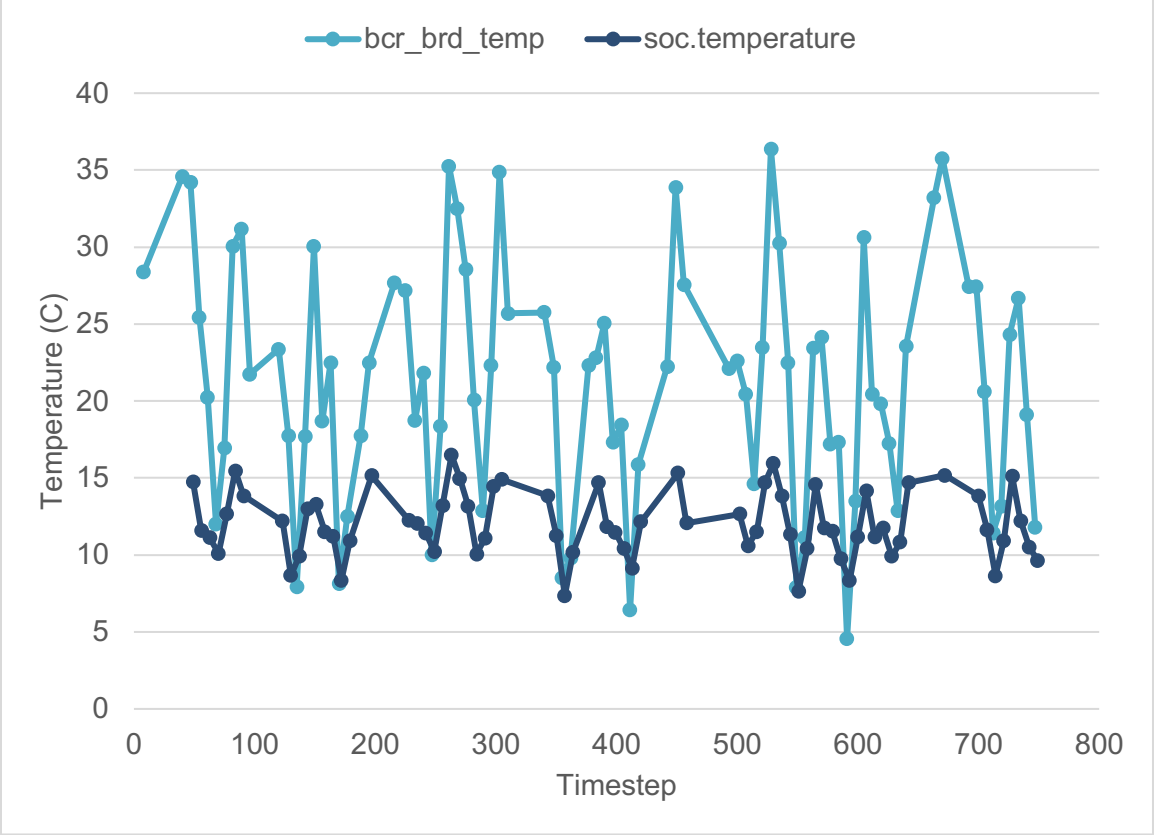


**Figure 9: SSO Satellite (FM79) Battery Charge Regulator (BCR) Board and System-on-Chip (SoC) Temperatures Only**[8]

Thermal models were made for three common sizes of small satellites that conform to the cube satellite (CubeSat) standard (See Appendix A for an overview of CubeSats): 1U (10x10x10 cm), 3U (30x10x10 cm), and 6U (30x20x10 cm). For each size, a simulation was run for an ISS orbit and for a 580 km sun-synchronous orbit (See Figure 10 for still image of CAD model of a 6U after Thermal Desktop processing and Figure 11 and Figure 12 for temperature output for that 6U as an example). These orbits were chosen due to their

[8] Data are given over a 24-hour period. “Timestep” is used as timesteps between data points varied by sensor and by time, resulting in data interpolation to provide comparable data points. Further information on that methodology can be found in Section Three.

popularity for small satellites. Simulation input criteria are summarized in Tables 3 to 5 in the Methodology section.

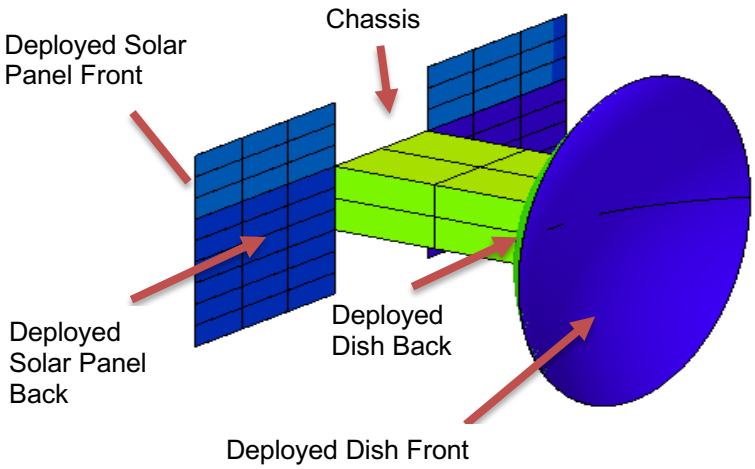


**Figure 10. 6U CAD Thermal Model**

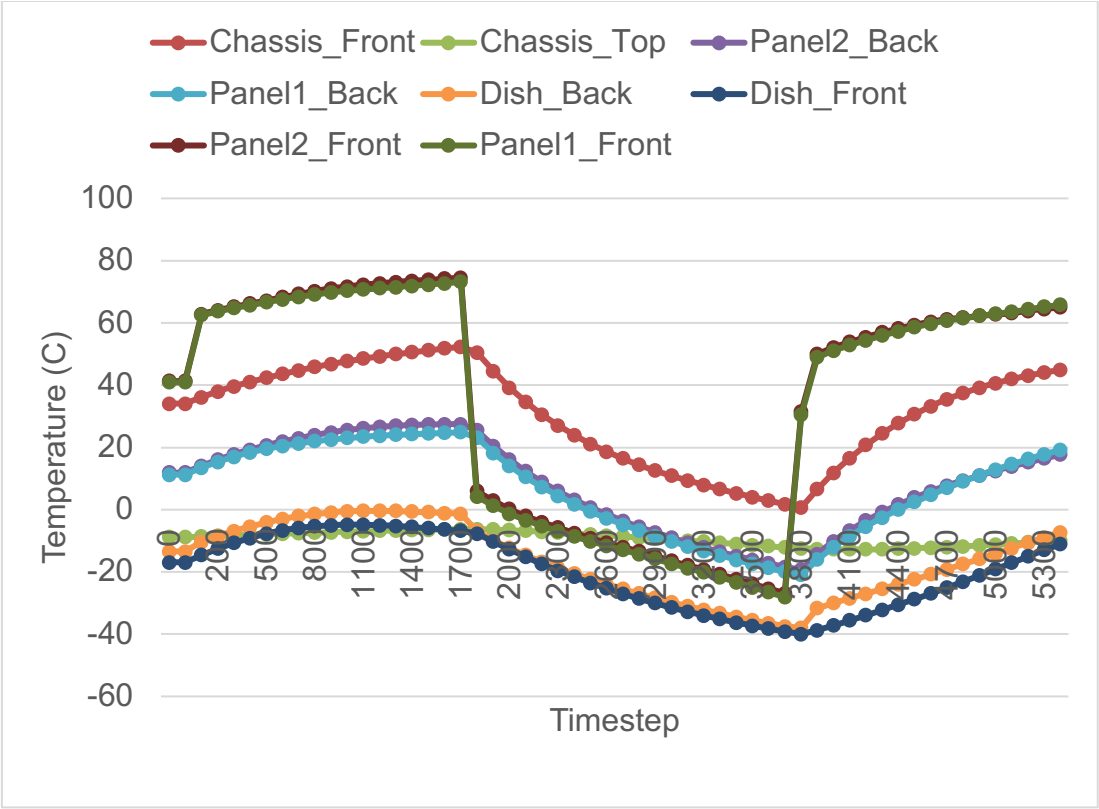


[9]

**Figure 11. 6U Thermal Model - All Deployables and Chassis Comparison Over Approximately One Orbit of 90 minutes (5400 seconds) [10]**

[9] There is a large temperature drop and then a spike when the satellite enters and exits eclipse. It is likely that in the event such a drop was seen for a planned satellite, the designers would change something about the design or change operational parameters to help smooth out that curve.

[10] One orbit was used instead of one day as was in the provided on-orbit data due to simulation run time costs. The orbit time of a satellite depends on a range of orbital dynamics factors but can be approximated by using just its altitude with a satellite orbiting closer to the Earth having a shorter orbit time than one orbiting farther away. The time for an orbit, also known as orbital period, is equal to $2\pi\sqrt{\frac{a^3}{GM}}$ where a is the semi-major axis (approximated as radius of Earth plus altitude above Earth), G is the gravitational constant, and M is the mass of the Earth. For an altitude of 400 km, this results in an orbital period of 92.5 minutes and for an altitude of 600 km, it is a period of 96.7 minutes. For satellites in LEO, the orbital time is therefore often approximated as 90 minutes (5400 in seconds).

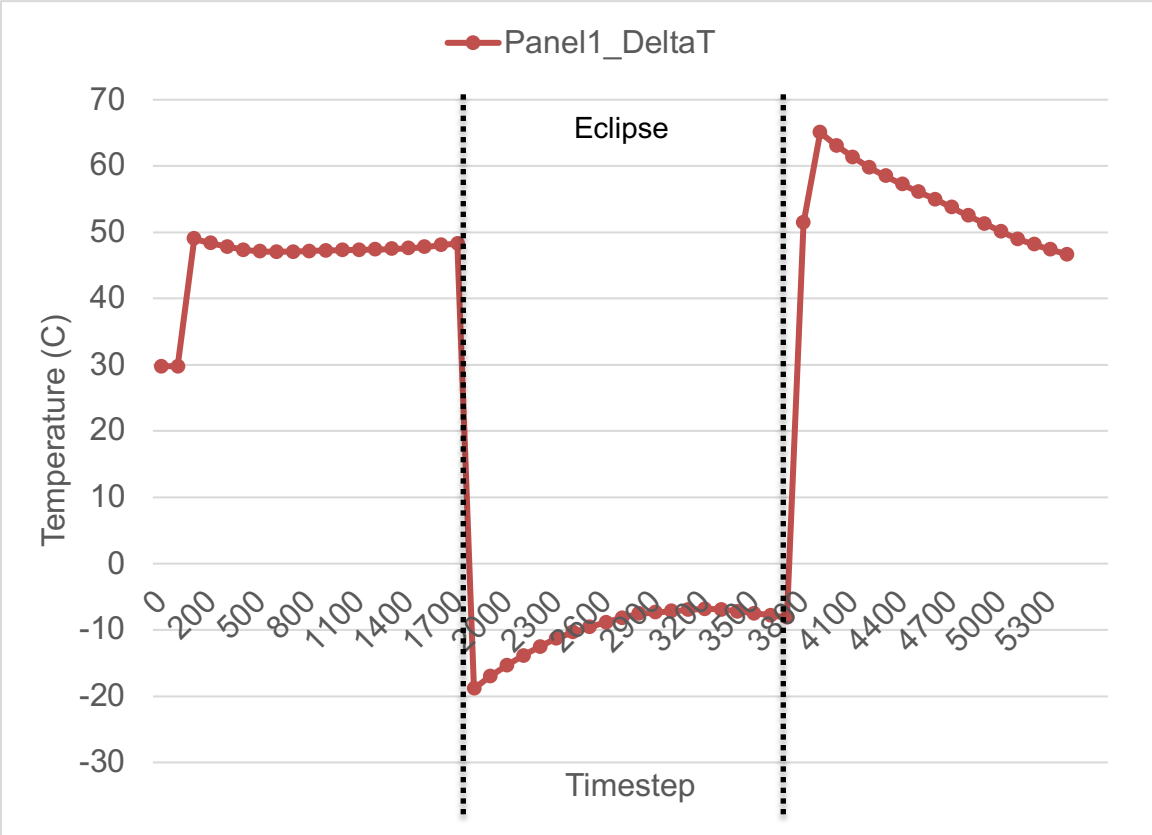


**Figure 12. 6U Thermal Model - Temperature Delta for One Solar Panel Over Approximately One Orbit of 90 minutes (5400 seconds)** [11]

After finding the temperature differentials, the power that could be generated by a TEG was estimated based upon a hypothesized 1U Bismuth-Telluride TEG (See Table 6 in Methodology section for characteristics). The assumptions made for the TEG were kept consistent across the analyzed data and the models.

The results ranged from 10.25 to 34 W/kg for the analyzed on-orbit data for internal and body-mounted components and from 15.83 to 154.99 W/kg for

[11] One orbit was used instead of one day as was in the provided on-orbit data due to simulation run time costs

deployed panels based upon the models. The results were significantly higher for ISS orbit satellites for both the analyzed data and the models.

These results compare favorably with the baseline comparison from the off-the-shelf solar panels. The hypothesized TEGs on solar panels, based upon on-orbit and modeled temperature differences, performed three to seven times better than the solar panels in some cases (See Table 1 for a summary of results).

| | **Average Power Per Mass (W/kg)** |
|---|---|
| **Comparison: Published Info for Off-the-Shelf Solar Panels** | 20.15 to 53.7 |
| Values below based upon analyzed/modeled temperature differences across a hypothetical TEG | |
| **On-Orbit Data - Spire Max Internal** | 34.00 |
| **On-Orbit Data - Dellingr Max Body-Mounted Panel** | 10.68 |
| **Thermal Model Max - Deployed Solar Panels** | 155 |

**Table 1. Summary of Analysis and Modeling Results**

TEGs would theoretically be able to produce power over more of an orbit compared to solar panels since while solar panels produced power goes to approximately zero when in the earth's shadow (See Figure 13 for model), there is thermal inertia in the satellite that would allow the TEG to continue to produce power, at least for a while, even in eclipse. Additionally, while solar panels produce power only with certain wavelengths of light (Ross & Hsiao, 1977), a

broader range of incident wavelengths will be converted into heat that a TEG could leverage depending upon the optical properties of the surface of the TEG.[12]

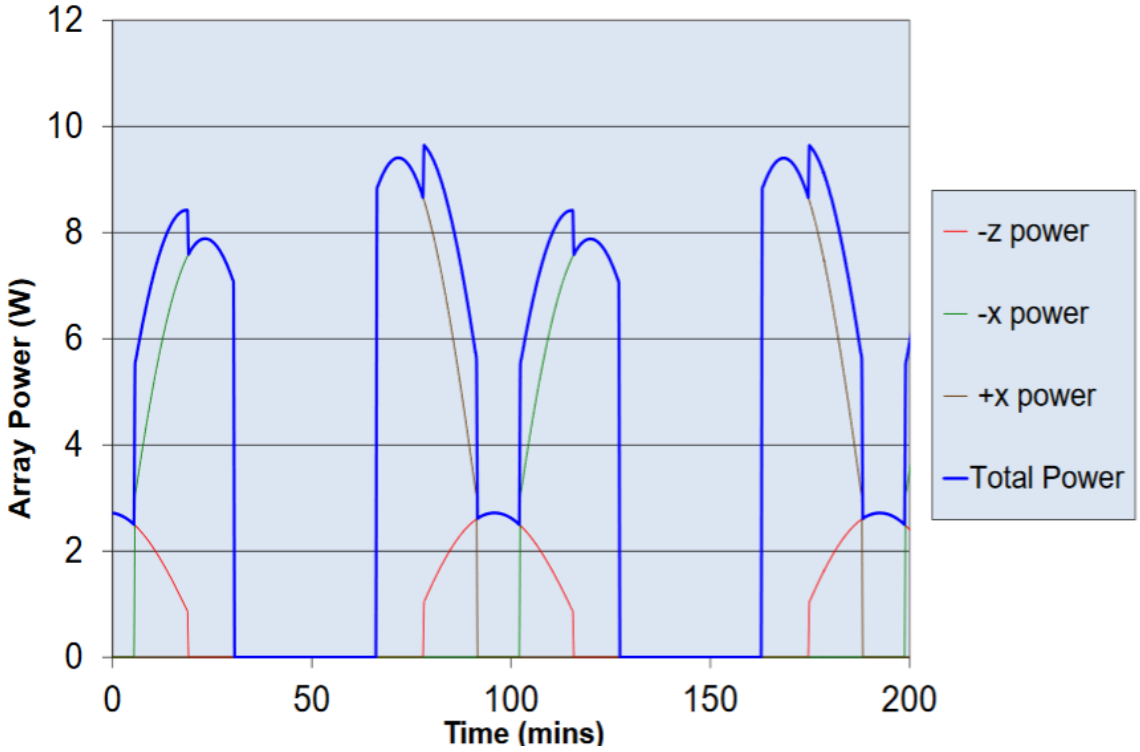


**Figure 13. Standard 3U Solar Panel Power Profile and Performance Across Three Faces (-Z, -X, and +X) [Reproduced from ClydeSpace (Clark & Kirk, 2012)]**

Despite those advantages, there are multiple caveats to the data which may cause TEG results to be too high. One, TEGs are generally 5-7% efficient (Lappas, Tsourdos, Kindylides, & Kostopoulos, 2019) while the solar panels used in the comparative sample range from 18 to 30% efficient (See Table 7 in Methodology section) so it would be reasonably expected that solar panels would

[12] The precise spectrum which are converted into heat by an object varies by multiple of the object's properties, including the molecules in the object as well as their physical state (Howell, Menguc, & Siegel, 2015)

outperform TEGs.[13] Two, in the analyses, the panel is modeled as essentially a perfect energy source since the TEG's impact on the thermal profile is not included. By placing a TEG on the panel to produce power, it will extract heat, some of which it will convert into electricity.[14]

Solar panels generally work better when they are cooler (See Figure 18 in Discussion and Conclusions section) so depending on whether the presence of the TEG produces a bump in the solar panel efficiency would depend on whether it was more efficient at transporting the heat away from the panel than the backing that would otherwise be there. Additionally, any increase in solar panel efficiency due to it being cooler would be at least partially offset by the decrease in power generation from the TEG due to the cooler hot side.

Even with the acknowledgement of those caveats, what the data analysis and modeling does show is that there seems to be a solid case for TEGs based on the expected specific power that they would provide due to environmental and dissipated heat. These results would likely provide enough incentive to motivate an operator to include a test TEG on their LEO satellite. Given the higher expected specific power and lower complexity of integration, placing a TEG on the back of a solar panel seems to be the best choice for a trial device.

---

[13] This comparison is not on equal footing as TEGs and solar panels each are able to convert different energy sources (thermal vs. specific electromagnetic waves). That distinction is explored in more depth in Section Five)

[14] A simple lab experiment was conducted using a resistive heating pad as the 'hot' solar panel and a block of aluminum as a heat sink for the TEG to reject heat into as a model for the change in thermal pathways a TEG would cause. A further description can be found in Section Five.

## Section Two: Background on Thermal Modeling

Thermal modeling involves predicting the temperatures and heat flows of a system given a design, a set of material properties, and a set of simulation criteria. A trade-off inherent in most modeling, including in thermal modeling, is between fidelity and time required for design plus simulation run time. Approximations made for this project to reduce design and simulation time are noted below and in the Methodology section.

For thermal modeling, there are two key sets of material properties: optical and thermophysical.

The optical properties are how the material responds to electromagnetic (EM) radiation. This is made up of four parts (See Figure 14 for a diagram of the four parts):

1. the radiation that reflects off like light off a mirror,
2. the radiation that is transmitted through like light through a window,
3. the radiation that is absorbed by the material,
4. and the radiation that the material emits.

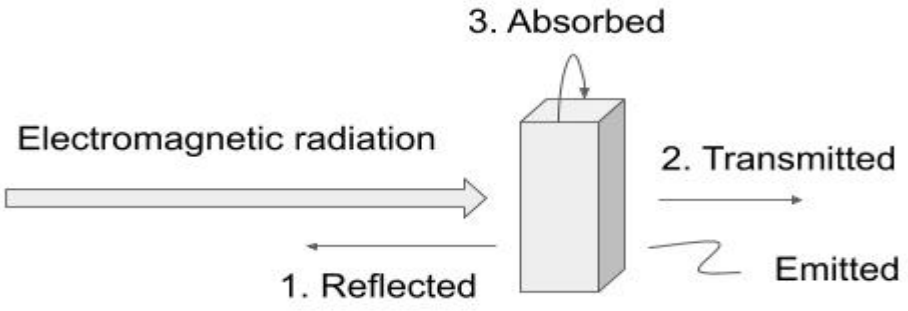


**Figure 14. Four Components of Material Optical Properties**

These properties vary by material and they vary for each material by the wavelength of the EM radiation as well as the temperature of the material. For the thermal modeling conducted in this project, solar absorptivity ($\boldsymbol{\alpha}$) and IR Emissivity ($\boldsymbol{\varepsilon}$) for each material without wavelength or temperature dependence was used as a first level approximation.

The second set of properties are thermophysical. These govern how the material responds to heat. It is made up of three key components (See Figure 15 for a diagram of the three components):

1. the thermal conductivity[15] which is how quickly heat flows through like how water can flow more quickly through a bigger pipe than an otherwise identical smaller one,
2. the specific heat which is how much energy must come in for a given quantity of a material to warm up,
3. and the density of the material which is how much mass is there per unit of volume.

[15] This is distinct from electrical conductivity although the two properties are highly correlated across many classes of materials.

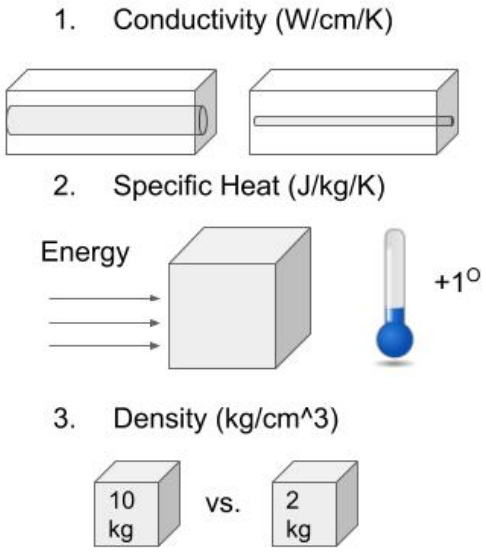


**Figure 15. Diagram of Components of Thermophysical Properties**

Like optical properties, thermophysical properties vary by material and by that material's temperature. And like the approximation used for those, material properties were assumed to be independent of temperature.

For the simulation criteria, it is not as simple to describe as the material properties due to the dozens of variables. A simulation can vary in run time, time step, number of times EM radiation is reflected, orbital parameters, time of year, and more. Decisions on key simulation criteria is explained in the Methodology section.

The software utilized in this project, Cullimore & Ring Technologies' Thermal Desktop, is based around modeling the temperature of a set of nodal elements with specified connections between them at different points.[16] In Figure

[16] Note: There are different ways of modeling (e.g. Finite Difference Methods (FDM) vs. Finite Element Methods (FEM)). The distinction and trade-offs are not covered here as different solvers/software are based on different methods. Due to an existing lab relationship, Thermal

16, the nodes can be seen in a portion of an example output from Thermal Desktop of a 1U satellite with deployed panels.

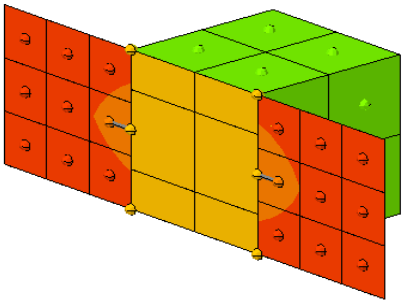

**Figure 16. Example Output Image of Model Using Thermal Desktop**

## Section Three: Methodology

The methodology was broken into a few intertwined threads:

- Obtaining and analyzing on-orbit satellite thermal data
- Thermal modeling
- Estimating specific power from a hypothetical thermoelectric generator (TEG) given the output of the on-orbit and thermal model data
- Gathering and analyzing solar panel data as a comparison

Overall, there were five different satellite types included in this project given that the three satellites from Spire were all 3Us of the same design (See Table 2

---

Desktop was chosen from the beginning. Given there was no trade-off analysis made in the research design, the criteria by which such a decision might have been made is not covered here.

for a summary of satellites used). The on-orbit data sources were supplemented with three different thermal models – a 1U, a 3U, and a 6U.

Those three sizes were chosen due to the relative popularity of them. While other configurations exist (e.g. 1.5U and 12U), they are not as frequently used as the 1U, 3U, and 6U (Nanosats Database, 2019).

| Name | Organization | Size | Image |
|---|---|---|---|
| Dellingr | NASA | 6U | 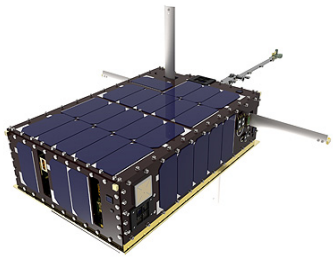 [17] |
| Lemur | Spire | 3U |  [18] |
| 1U Thermal Model | N/A | 1U | 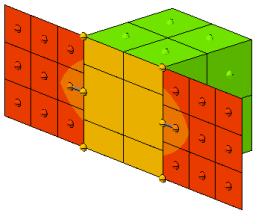 |
| 3U Thermal Model | N/A | 3U | 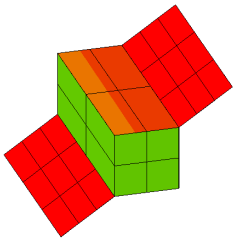 |
| 6U Thermal Model | N/A | 6U | 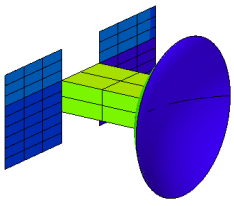 |

**Table 2. Satellites in Analysis and Thermal Models**

[17] (NASA)
[18] (Spire)

### *On-Orbit Thermal Data Analysis*

Attempts were made to source on-orbit thermal data from satellite operators to analyze and to help ground-truth the thermal models. Spire and NASA generously provided select on-orbit thermal data.

The key part of this research was to quantify the potential opportunity for a TEG. That meant looking for large temperature differences. The overall process for each data set was:

1. Clean and standardize the data
2. Determine the “hottest” and “coldest” points in the spacecraft
3. Calculate the temperature difference between those two points over time

Key decisions made in cleaning and standardizing the data were:

- **Eliminate erroneous values.** Data had numerous values that appeared spurious - for instance, a relatively stable temperature reading jumping more than 100% in one-time step and then going back to the previous reading at the next time step. Values that were 100% or more different from than the value before and after it were discarded
- **Standardize timing.** The frequency of temperature sensor readings varied by sensor and the timesteps between readings varied. To be able to make comparisons across time, there needed to be a way to match points. Straight-line interpolation between points was used to provide matching points.

- **Make proximity assumption.** No CAD document was provided for the interior of the satellites. Without that, it's unknown how far or close components are to each other and therefore what the feasibility is of putting at TEG in between them. By necessity rather than due to a belief that this is true it was assumed for this analysis that all internal components had an equally viable thermal pathway between them for a TEG.

### *Thermal Modeling*

Since the on-orbit thermal data was provided for the internals of the satellites but not deployables[19] and because deployables were expected to present the greatest opportunity given that one side could be facing the sun while the other would be facing the cold of space, the focus of the modeling was on deployables.

A trade-off in modeling is fidelity vs. time for the design plus simulation. Even seemingly minor design or simulation parameter changes can result in unwieldy simulation times[20] while causing no meaningful change to the results. An example trade-off can be seen by looking at the models in Table 2 and specifically how the faces of each model are segmented. The more segments per

[19] Dellingr does not have deployed panels. Spire satellites do but the thermal data for them was determined too unreliable to even provide to the researcher by the company.
[20] While typical simulation times were on the order of 30 seconds to a couple of minutes, even seemingly minor changes to models or simulation parameters could cause a single run time to jump to hours.

face, generally the more true-to-life the result but including those additional segments increases the computational time.

As noted at the start of the Methodology section, there are dozens of variables that can be tweaked. Variables that were determined to be key and sufficient to replicate the modeling results are summarized in Tables 3, 4, and 5 for the simulation input criteria, optical properties, and thermophysical properties respectively. A few key decisions are explained below:

- Each model face was split into no more than a 3x3 grid except for the 6U solar panels which were modeled as three 3x3 grids connected to reflect that such panels are generally three separate 3x1U panels. Trial runs were conducted with a finer mesh and the results were not appreciably different. Given the high simulation run time cost associated with any increase in mesh density and minimal change in output, a looser mesh was kept.
- Beta angles were calculated for July 14th, 2019 to correspond with the date of data provided by Spire. Beta angles take multiple factors into account to produce a value that expresses how much time a satellite will spend in the sunlight and that value will change over the course of a year for LEO satellites.
- Modeling focus was on the thermal profile of deployables so to lower modeling and simulation time costs, the chassis was modeled as a box with a constant 293.15 K source at the center to approximate a satellite

kept on and in operating temperature range. This value is within the range seen in the on-orbit thermal data. The chassis was then connected to the deployables via two-way conductors.

- Satellites were modeled body-nadir pointing, the solar panels were put to angle directly out in the +Z direction. No operational maneuvers were modeled and the solar panels themselves were not independently articulated.
- Optical properties of materials were wavelength independent

| | Case 0: Sun-Synchronous Orbit | Case 1: International Space Station Orbit |
|---|---|---|
| **Beta Angle (degrees)**[21] | -26.44 | 33.66 |
| **Altitude** | 580 | 410 |
| **Solar Flux (W/cm^2)** | 0.1354 | 0.1354 |
| **Albedo** | 0.35 | 0.35 |
| **IR Planetshine (K - Blackbody)** | 250[22] | 250 |
| **Satellite Orientation** | Body nadir-pointing (-Z) | Body nadir-pointing (-Z) |
| **Solar Panel Orientation** | +Z | +Z |
| **Space Node Temperature (K)** | 2.73 | 2.73 |
| **Calculation Method** | Monte Carlo | Monte Carlo |
| **Random Number Seed Control** | Unique random number seed at start of calculations | Unique random number seed at start of calculations |
| **Oct Cells** | Oct-tree used to accelerate calculations (Max oct-tree subdivisions: 7. Max surfaces per cell: 8) | Oct-tree used to accelerate calculations (Max oct-tree subdivisions: 7. Max surfaces per cell: 8) |
| **Electromagnetic Radiation Wavelength Dependence** | None | None |
| **Rays Per Node** | 5000 | 5000 |
| **Fast Spin** | No fast spin calculations | No fast spin calculations |
| **Simulation Time (seconds)** | 5400[23] | 5400 |

**Table 3. Thermal Model Simulation Input Criteria**

[21] Calculated for July 14th, 2019 to correspond with date of on-orbit thermal data from Spire. The amount of time a satellite spends in the sun depends on the satellite's inclination and its right ascension of ascending node as well as the sun's declination and right ascension. Those values vary over the course of the year.

[22] 0.02215 W/cm^2 in terms of Flux

[23] Chosen as it is approximately one orbit. While the orbit for the SSO will be longer than ISS, to keep the dataset size consistent, an approximate time for one orbit was chosen.

| | Solar Absorptivity | IR Emissivity | α/ε |
|---|---|---|---|
| **Black Anodized** | 0.65 | 0.82 | 0.793 |
| **MLI Surface** | 0.15 | 0.05 | 3 |
| **Mylar Film** | 0.14 | 0.28 | 0.5 |
| **Solar Cells** | 0.82 | 0.85 | 0.965 |
| **White, zinc oxide** | 0.16 | 0.93 | 0.172 |

**Table 4. Simulation Optical Properties**

| | Conductivity (W/cm/K) | Density (kg/cm^3) | Specific Heat (J/kg/K) | Effective Emissivity |
|---|---|---|---|---|
| **Honeycomb** | 1e-5 | 1e-06 | 544 | 0.05 |
| **MLI, 7-layer** | 0.0003 | 1e-06 | 0 | 0.05 |
| **Mylar Film** | 0.15 | 0.00139 | 1172.3 | |
| **Solar Cell** | 0.01 | 1e-06 | 1 | 0.45 |
| **Structure** | 1.67 | 0.0027 | 896 | |

**Table 5. Simulation Thermophysical Properties**

### *Estimated Specific Power from Hypothetical TEG*

The temperature difference profiles from the on-orbit and model data analysis were then used as the basis for estimating the likely average power output from a TEG in between those hot and cold sources. A key part of TEG effectiveness is how many thermoelectric pairs (A n-doped pellet and a p-doped pellet) there are. To estimate how many pairs could fit on a 1U panel (10x10 cm), a commercial TEG[24] was used (See Table 6 for values used).

The output power was calculated as follows:

[24] Commercial and non-space-rated TEG chosen from Laird (Laird Thermal Systems, Inc.)

$$Open\ Circuit\ Voltage\ (Voc) = \left(Temperature\ Difference\ (\Delta T)\right) * \left(Number\ of\ Thermocouple\ Pairs(N)\right) * (Seebeck\ Coefficient)$$

$$Power\ \max\ (Pmax) = \frac{\left(Open\ Circuit\ Voltage\ (Voc)\right)^2}{4 * Internal\ Resistance\ (Rin)}\ ^{25}$$

The Pmax was considered equal to output power at each time step. An average across all time steps was taken. As can be seen, where different possible assumptions could be made, the one that would maximize expected power was chosen (e.g. with Pmax=P). This generous approach to assumptions was taken as the purpose of this portion of the project was to determine whether an opportunity might exist and therefore looking at best possible performance that could be realistically expected was used as a guiding approach. These results however should not be taken as indicative of performance for a particular mission and analysis would need to be done for specific candidate missions before a TEG was incorporated.

[25] Assumed that Internal Resistance was equal to Load Resistance (Rin=RL). This maximizes the predicted output power. A maximum power point tracking device, essentially a sensor and a variable resistor, can be used to help ensure Rin=RL.

| | |
|---|---|
| **Number of Thermocouple Pairs (N)** | 1250 |
| **Seebeck Coefficient (V/K)** | 0.00053[26] |
| **Internal Resistance (Ohms)** | 11 |
| **Mass (kg)** | 0.1075 |

**Table 6. Thermoelectric Generator Characteristics Used for a Hypothetical 1U Panel**

*Comparison to Next Best Alternative*

Whether a TEG is "good" or "bad" is only in relation to what the alternative is. At a high-level, a satellite's power budget is power consumption vs. power generation. If the developed power budget is negative, meaning the satellite will not generate enough power for what it wants to do, then satellite designers have two options: reduce power consumption or increase power generation. To reduce power consumption, a designer or operator could:

- Use more power efficient components
- De-scope certain functions (e.g. remove a second imager)
- Change the operational plan to reduce power consumption

Each of these options generally increases cost and/or reduces the value that the mission provides.

The other avenue is to increase power generation. Solar is the source of power now for LEO satellites. Therefore, the default option is to put solar panels on more surfaces or procuring more efficient solar panels, if possible. If there is no more surface area on the chassis, that means introducing deployment

[26] Approximate Seebeck Coefficient for Bismuth Telluride. Actual coefficient depends on manufacturing process and temperature - (Matthes, et al., 2018)

mechanisms which can be progressively more complicated to increase the total surface area. See Figure 17 for an image of a 3U satellite with deployed solar panels as an example of what these can look like.

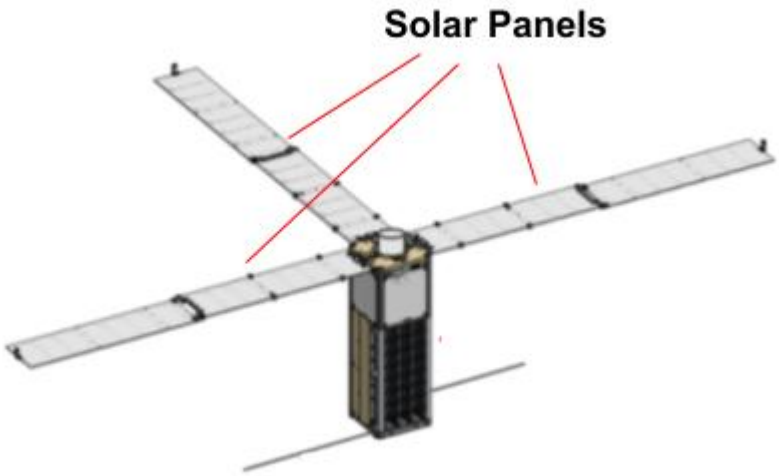


**Figure 17. CAD Image of a 3U Satellite with Deployed Solar Panels (Analytical Space, Inc., 2019)**

If the decision is made to increase power generation as opposed to reducing consumption, TEGs can be compared to the next best alternative of adding solar panels. Space-rated solar panels vary in effectiveness and therefore five solar panels designed for CubeSats were considered to provide an approximate range to compare TEGs against.

From the published datasheets as summarized in Table 7, the mass, max power, efficiency, and operating temperatures can be drawn out. Part of the time, LEO satellites will be in Earth's shadow but that amount of time will vary (Longo & Rickman, 1995). When it is in earth's shadow completely, the solar incident energy goes to zero. As a rough approximation, calculations were made

assuming half of the time the solar panels were hitting max power and half they were producing zero power due to being eclipsed for an average on-orbit power of 50% max power. That average on-orbit power was then divided by the mass of a 1U panel assembly to provide a specific power in watts per kilogram (See Table 7 for solar panel comparisons)

| | EXA Panel (Low-Cost Version)[27] | EXA Panel (High-Power Version)[28] | Space Quest[29] | EnduroSat [30] | ISI Space[31] |
|---|---|---|---|---|---|
| **Mass (kg)** | 0.067 | 0.067 | 0.01 | 0.044 | 0.05 |
| **Max Power (W)** | 2.7 | 7.2 | 0.88 | 2.4 | 2.3 |
| **Estimated Average Power (W)[32]** | 1.35 | 3.6 | 0.44 | 1.2 | 1.15 |
| **Efficiency (%)** | 19 | 30 | 18 | 29.5 | 30 |
| **Operating Temp. Range (K)** | 193-403 | 193-403 | 183-363 | 233-378 | 233-398 |
| **Power/Mass (W/kg)** | **20.15** | **53.7** | **44** | **27.2** | **23** |

**Table 7. 1U Solar Panel Comparisons**

## Section Four: Results

The key results are summarized in Table 8. As a baseline comparison, the specific power of CubeSat solar panels ranges from 20.15 to 53.7 watts per kilogram. The max internal heat differences based upon the on-orbit data results in specific powers of roughly 10 watts per kilogram for three out of the four

[27] (Agencia Espacial Civil Ecuatoria, 2016)
[28] (Agencia Espacial Civil Ecuatoria, 2016)
[29] (SpaceQuest, 2016)
[30] (EnduroSat)
[31] (ISI Space)
[32] This is estimated as 50% of the max power. The actual on-orbit average power would vary by orbit and orientation of the panels.

satellites. This compares unfavorably to the solar panels although within an order of magnitude. However, the Spire satellite in an ISS orbit had larger temperature differentials resulting in a theoretical max specific power of a TEG inside of 34 watts per kilogram, making it competitive with solar panels.

For the thermal models which were focused on deployables, the results for the SSO satellites ranged from a max of 15.83 to 47.59 watts per kilogram. Within the range of what solar panels are providing. However, for ISS orbit satellites, results ranged from 103.63 to 154.99 watts per kilogram. That is two to three times as high as the best performing CubeSat solar panel.

| # | Source | Mass for 1U Panel (kg) | Average Temperature Difference (K)[33] | Average Power Over Orbit (W) | Specific Power (W/kg) |
|---|---|---|---|---|---|
| **Solar Panel Comparisons (From Vendor Published Materials)** | | | | | |
| 1 | EXA Panel (Low-Cost Version) | 0.067 | N/A | 1.35 | 20.15 |
| 2 | EXA Panel | 0.067 | N/A | 3.6 | 53.7 |
| 3 | SpaceQuest | 0.01 | N/A | 0.44 | 44 |
| 4 | EnduroSat | 0.044 | N/A | 1.2 | 27.2 |
| 5 | ISI Space | 0.05 | N/A | 1.15 | 23 |
| **On-Orbit Data Thermal Data for Thermoelectric Generator** | | | | | |
| 6 | Spire SSO 1 Max Internal ΔT | 0.1075 | 9.21 | 1.10 | 10.25 |
| 7 | Spire SSO 2 Max Internal ΔT | 0.1075 | 8.30 | 1.18 | 10.98 |
| 8 | Spire ISS 1 Max Internal ΔT | 0.1075 | 16.28 | 3.66 | 34.00 |
| 9 | Dellingr - Max ΔT of Body-Mounted Panel | 0.1075 | 1.44 | 1.15 | 10.69 |
| **Thermal Models for Thermoelectric Generator** | | | | | |
| 10 | 1U ISS Orbit | 0.1075 | 23.63 | 12.00 | 111.58 |
| 11 | 1U Sun-Synchronous Orbit | 0.1075 | -1.04 | 3.74 | 34.83 |
| 12 | 3U ISS Orbit | 0.1075 | 23.88 | 11.14 | 103.63 |
| 13 | 3U Sun-Synchronous Orbit | 0.1075 | 3.77 | 1.70 | 15.83 |
| 14 | 6U ISS Orbit | 0.1075 | 28.50 | 16.66 | 154.99 |
| 15 | 6U Sun-Synchronous Orbit | 0.1075 | -0.26 | 5.12 | 47.59 |

**Table 8. Summary of Key Results**

[33] Power was calculated as $P=V^2/R$. By squaring the voltage, the result is always positive. The voltage depended upon the temperature difference as related by the Seebeck coefficient (units: Volts/Kelvin). This means that for cases where there were lots of inversions (hotter side becoming the colder side), the average temperature difference could be dragged down or even go slightly negative.

## Section Five: Discussion and Conclusions

Before discussing TEGs compared to solar panels, there is one outcome to discuss that was unexpected – the large TEG performance difference found between ISS and SSO satellites. That difference is consistent between the models as well as the on-orbit thermal data.[34] Possible reasons for this include the different amounts of solar illumination due to the different inclinations and closer proximity to the Earth which would result in higher incidence of albedo and IR planetshine. Teasing out the exact reason was determined to be tangential to the main thrust of this part of the project and so was not explored.

Turning to the main thrust of the results, at first glance, these results are very promising. At a minimum, TEGs seem competitive with solar panels if not a better option.

To deal with one idea immediately – these results are suggestive of the possibility of completely removing solar panels and exclusively using TEGs. Given non-radioactive TEGs are relatively unproven on spacecraft, it would be unwise from a risk perspective to rely on them as an only option until they've been proven as a secondary system.

Placing a TEG into or onto a system will change that system. At minimum, placing a TEG will change the thermal mass profile and a TEG is unlikely to have the same thermal conductivity as what would otherwise be there on a satellite.

[34]Although the sample size is small with only one ISS satellite in the sample.

And if placed on the back of a deployed panel, TEGs have higher thermal conductivity than the approximate value of zero for space.

This higher thermal conductivity could mean that the TEG would have the effect of adding a cooling effect. Solar panels generally work better when cooler (See Figure 18 for a voltage vs. temperature plot for an example solar cell showing that lower temperatures result in higher output voltages). Therefore, a TEG could provide a double power benefit on the back of a solar panel by producing power and by increasing the efficiency of the solar panel it is attached to if it keeps the solar panel cooler than it otherwise would be.

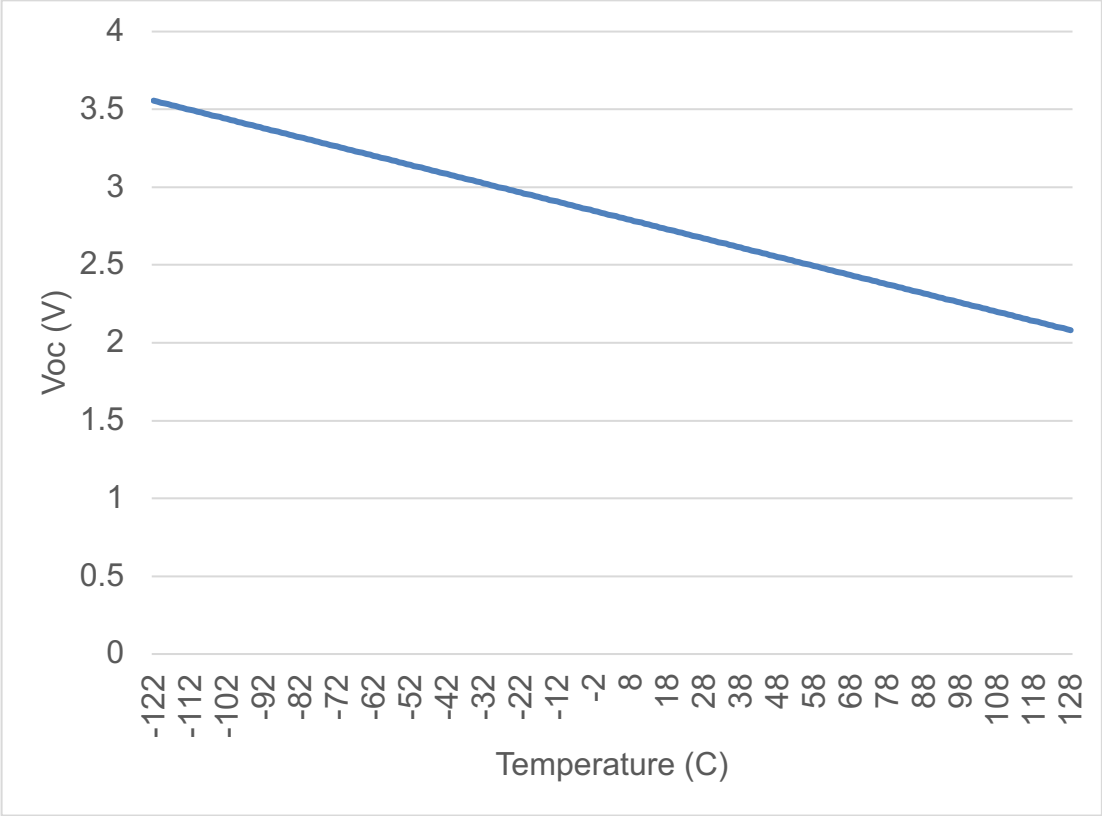


[35]

**Figure 18. Solar Panel Expected Open Circuit Voltage vs. Temperature**

[35] Based on data from (SolAero Technologies, 2016). The relationship as given is linear but that may not be true at extremes.

A simple lab experiment was done to explore the effect of adding a TEG. A resistive heating pad as the ‘hot’ solar panel and a block of aluminum as a heat sink for the TEG to reject heat into (See Figure 19). The pad was heated up with the power inputted and temperature recorded. Once it had reached a steady state, the TEG with the aluminum block on top of it was placed on the pad. There was no direct contact between the resistive pad and the aluminum block heat sink. As expected, the pad drew more power to maintain the same temperature (See Figure 20 for graph of power into the pad and power out from the TEG). From the perspective of the pad (and a solar panel), the fact that the TEG converts heat to electricity is insignificant, it just sees a thermal pathway and heat sink that has a certain temperature, thermal conductivity, specific heat, density, and mass.

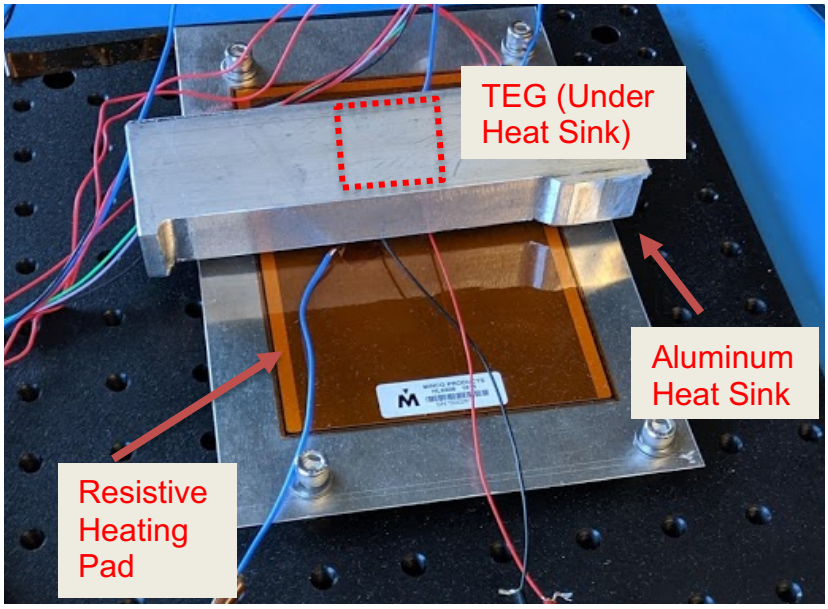


**Figure 19: Thermal Flow Lab Experiment Set-up**

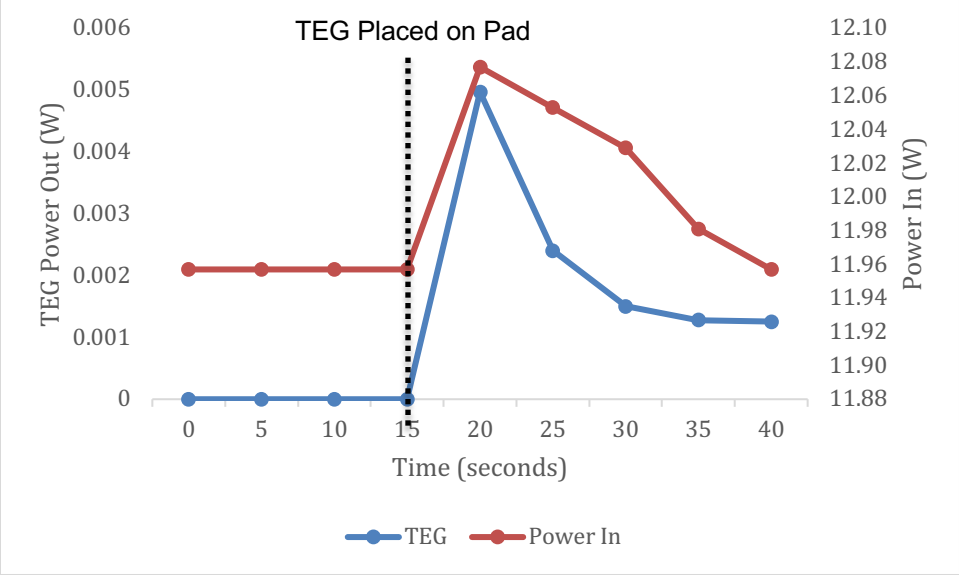


**Figure 20: Measured TEG Output Power on Resistive Heating Pad[36]**

There are possible reasons for a TEG to have higher performance than a solar panel. One, there is inertia in the power generation of a TEG due to thermal mass. Even after a heat source is removed, a mass will stay warm and then slowly reach equilibrium with its environment. Solar panels however go to zero power generation whenever the photon source (e.g. the sun) is blocked or removed. This means that a TEG could produce power over more time of an orbit than a solar panel.

Two, solar panels are only able to utilize specific wavelengths of EM radiation[37] while a broader range of wavelengths can be absorbed by materials

[36] The key takeaway relates to the time close to the placement of the TEG before and after. Therefore, future data points were omitted that would have lengthened the graph and made the key time period harder to read. To note on long-term behavior, over time heat is conducted across the TEG and the "cold" side warms up. As the cold side temperature approaches the hot side temperature, TEG output power goes to zero. The power-in will return to steady state once the thermal mass placed upon it (TEG plus aluminum heat sink) stabilize in temperature.

and converted into heat.[38] Most simply, this reduces the sources of energy for solar panels. While thermal energy comes from solar flux, albedo, IR planetshine, and generated heat as described in the Introduction, solar panels only leverage solar flux and albedo.

TEGs also have the potential to generate power in otherwise underutilized spots on a satellite. For instance, putting solar cells on the back of an existing deployed solar panel is unlikely to make much sense as only one side can be pointed at the sun at one time but a TEG can be placed there.

Along the lines of underutilized locations, the internal TEG results should be approached cautiously since the internal designs of the satellites were not provided for this study. Therefore, it is not known whether a TEG could fit in between the identified “hot” and “cold” components.

One concern which casts doubts on these results is that TEGs are less efficient as mentioned in Section One when compared to solar panels (~5–7% for TEGs compared to ~18–30% for solar panels). This efficiency gap on the face may be smaller in practice due to a variety of factors including that TEGs convert thermal energy while solar panels convert EM radiation but based on a first-pass, it is suspicious that the TEGs would potentially generate multiple times the amount of power as a solar panel as suggested by the results from the modeling

---

[37] This is true for solar panels (Ross & Hsiao, 1977) although work is being done on improving the range of wavelengths absorbed (Lumb, et al., 2017)

[38] The precise spectrum which are converted into heat by an object varies by multiple of the object’s properties, including the molecules in the object as well as their physical state (Howell, Menguc, & Siegel, 2015)

as can be seen comparing the highest specific power for a solar panel in line 2 of Table 8 and the highest specific power for a modeled TEG in line 14 of Table 8.

A likely larger issue is that TEGs only generate power so long as there is a heat differential. The thermoelectric pellets are thermally conductive and therefore will equalize in temperature over time given a heat source unless heat is being conducted away sufficiently on the cold side to keep it cold. This issue of reliably keeping the “cold side” cold is what led one team of researchers to propose a fluidics system to carry heat away (Lappas, Tsourdos, Kindylides, & Kostopoulos, 2019). Introducing a fluidics system increases complexity, thus negating one of the benefits of a TEG compared to progressively more complicated solar panel deployment mechanisms.

There is also the issue of the large temperature swings seen in the thermal models (for example in Figure 12) being perhaps unreasonably large. If those rapid temperature changes were anticipated, design or operational plan changes would likely be made as such rapid heating or cooling would likely cause unwanted stress on the components. This highlights one of the potential issues with TEGs — the large temperature differences that are valuable for TEGs can be otherwise undesirable.

A final caveat is that there were a host of assumptions that were made as outlined in the Methodology section. On an individual basis, many of them may not broadly hold. Therefore, these results should not be read as directly indicative of what a satellite incorporating a TEG would get in power generation

but rather it is suggestive that it is worth exploring the option.

Overall, the results from this analysis with specific power values peaking as high as 155 W/kg in line 14 of Table 8 also agrees in a broad sense with previous work done by others with specific power values as high as 125 W/kg for a conceptual TEG found by Lappas, et. al. (Lappas, Tsourdos, Kindylides, & Kostopoulos, 2019) and idealized values of 700 W/kg and 52 W/kg for two different TEG materials found by Lukowicz et. al. (Lukowicz, Abbe, Schmiel, & Tajmar, 2016). This project extends previous work with analysis of on-orbit thermal data and more detailed thermal models across a variety of common mission parameters.

In summary, even if the applicability of any assumption to a particular mission may not hold, what the results of the analysis and modeling show is that there is a promising potential opportunity for LEO small satellites to incorporate TEGs to augment power generation. The back of deployed solar panels is the highest value candidate location due to simpler integration and higher temperature gradients.

# CHAPTER TWO: DESIGN

## Section One: Summary of Design Efforts

This part of the project flowed from the opportunities identified in Chapter One. Based upon the findings, a different tack was taken than initially expected.

One potential opportunity that was considered initially was to design a thermoelectric generator (TEG) to take advantage of internal heat flows. Given the packed internals of small satellites, the likelihood was low of being able to insert standard planar TEGs without disrupting the rest of the satellite and potentially disturbing the target heat flows. Therefore, the idea of being able to design bespoke TEGs that fit into unusual shapes was initially considered. The geometric complexity and manufacturing costs would likely be prohibitively high using most manufacturing methods, but the added cost of geometric complexity is greatly reduced with additive manufacturing. Work has been done[39] on developing the ability to use the additive manufacturing set of techniques to make TEGs but the techniques are still at their early stages and the raw materials as well as the necessary equipment is hard to access. While this still seems like a potentially promising future approach, that path was not followed since the internal designs of the satellites were not known and the largest opportunity proved to be the planar surface of solar panels.

Due to the low-relative cost of designing and manufacturing printed-circuit boards (PCB) as well as the shared commonality of the material FR-4 being used

[39] For example: (Kim, et al., 2018)

as a backing of solar panels in space as well as the foundation for PCBs, PCBs were chosen as the manufacturing approach. PCBs also have low geometric complexity costs in 2D allowing for easy variations in architectures.

A standard single PCB would not have been enough as the thermoelectric elements need to be mounted with connections on the top and on the bottom. Therefore a 'PCB sandwich' approach was used whereby the thermoelectric elements were placed in between two PCB boards and the entire assembly was soldered together (See Figure 21 for image of assembled PCB).

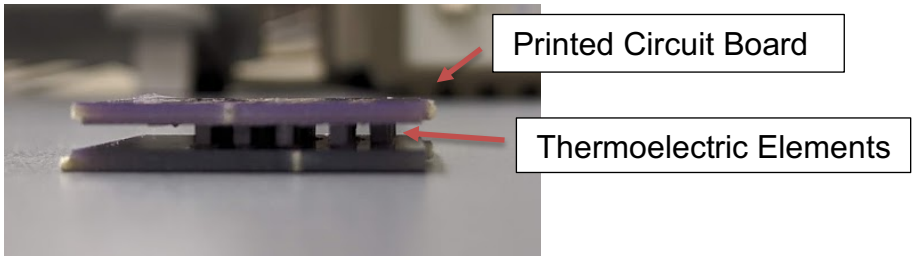


**Figure 21: Assembled PCB Sandwich Thermoelectric Generator**

As a part of this project, the manufacturing approach was validated and several design configurations were considered. The design of a full-scale functioning prototype is left as a future direction.

## Section Two: Design Approach

### *Manufacturing Approach*

Multiple manufacturing approaches were considered. While options, including additive manufacturing, were considered if the greatest thermal opportunities were shown to require geometrically complex TEGs to harvest the

energy, ultimately the analysis and modeling pointed towards the use of planar TEGs on the back of deployed solar panels as the greatest opportunity as can be seen from the higher specific power values for placement on deployed panels in Table 8 lines 10 to 15 compared to internal and body-mounted panel values in lines 6 to 9 of Table 8.

It was desired to be able to trial different configurations of the thermoelectric elements as well as to use materials that have been shown to work in the space environment. For those reasons and due to the relative low cost, printed circuit boards (PCB) were chosen.

### *Designs*

Similar to the factors impacting the manufacturing approach, the design was constrained to flat panels.

Traditional commercial TEGs are laid out in a square grid pattern (See Figure 22 for a diagram). However other designs are possible. It's possible to vary the spacing of that grid or to do other geometric designs including spirals or concentric circles. Other options were explored in initial small-scale prototyping (See Figure 23 for initial prototypes) and the idea for a non-grid structure was driven by research done on novel configurations for thermal cloaks (Han & Qiu, 2016).

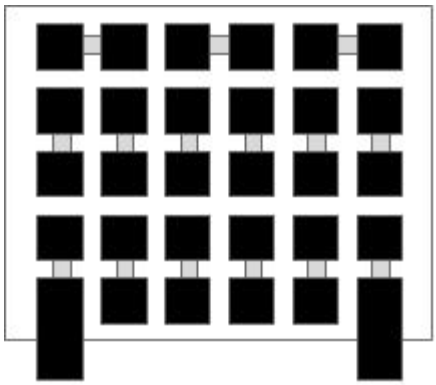

**Figure 22. Diagram of a Grid Thermoelectric Generator**

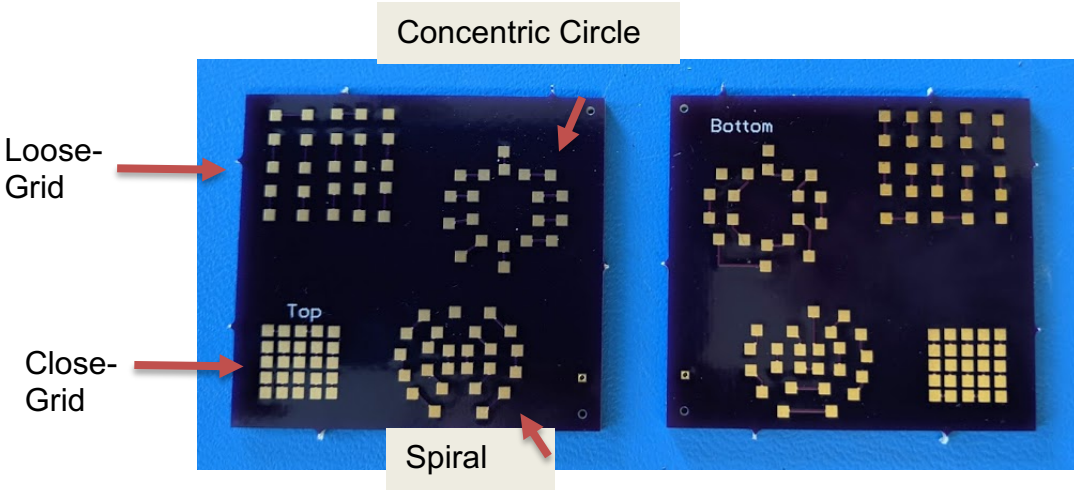


**Figure 23. Prototype PCB (5 cm x 4.6 cm) with Four Configurations**[40]

*Assembly Process*

The PCBs were designed using EagleCAD and surface mount pads (1.6x1.6mm) were placed to accommodate the dimensions (1.4x1.4x1.6) plus a margin of the procured thermoelectric elements (Bismuth Telluride from Wuhan Xinrong New Materials Co., Ltd). Boards were ordered through OSH Park with a

[40] Note: The spacing of elements was varied to help determine the minimum possible distance between elements possible without shorting connections. This trial was done as the researcher did not have access to a pick and place machine with defined specifications but rather had to assemble it by hand.

2-sided approach (the ‘Top’ designs were on one side of every board and the ‘Bottom’ designs were on the other side) to cut down on costs. The boards came with four possible designs on them (See Figure 23). Upon receipt, the boards were broken into their four panels by straight-line scoring the PCB and snapping the panels apart. Solder paste (Kester NXG1 – Lead Free) was applied using a stencil (Polyimide Film 3mil from OSH Stencils). Any excess solder was removed before each of the thermoelectric elements was placed by hand using tweezers. The assembly was then placed into a reflow oven to solder it together. This was done once “open-face” without a PCB placed on top (See Figure 24) to allow for verification of conductive pathways. For the second iteration, solder paste was applied to the ‘Top’ PCB with a stencil and that PCB was placed on top of the thermoelectric elements that had been placed on the soldered pads of the ‘Bottom’ PCB. That whole assembly was then placed into the reflow oven (See Figure 25 for assembled TEG).

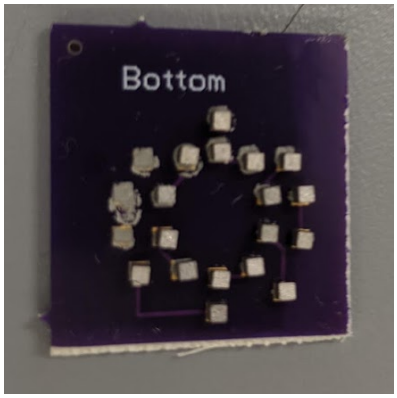


**Figure 24. Open-Face of TEG with Thermoelectric Elements on PCB**

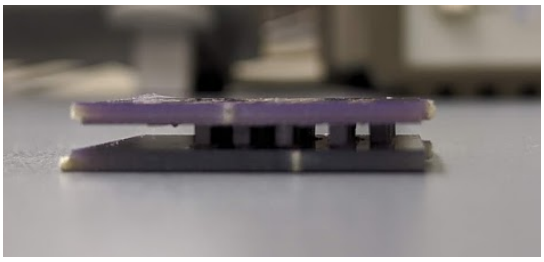

**Figure 25. Assembled TEG**

## Section Three: Results and Discussion

Using a multimeter, it was possible to verify that the conductive pathways through the PCB, thermoelectric elements, and solder performed as expected. However, shorts prevented the construction of a complete device. For the spiral, concentric circle, and close-grid designs, some or all pads were too close together and resulted in solder shorts. For the loose-grid design, shorts resulted due to the door mechanism of the reflow oven. The oven's door, which was connected to the tray for the PCB, had a latch at the end of the door track to keep the door closed. When the door slides past that latch, the door slightly jumps. Since the door was attached to the tray which held the PCB, that caused the assembly to shift, causing shorts to form.

Based upon the lessons learned regarding spacing of the pads and the need for a mechanism to keep the PCBs aligned while closing the oven door, a follow-up TEG was designed. The design was 8x8 cm[41] with a 3.6 mm gap in between each element, a 6.2 mm buffer around the edge, and a through-hole in

[41] Goal was 10x10cm to align with 1U but the software (EagleCAD 7.7.0) wouldn't allow PCBs larger than 8x10cm. To have a square form factor, 8x8 cm was chosen to get as close as possible given the software limitation of 10x10 cm

each corner to allow for fasteners to keep the PCBs aligned during reflow oven soldering (See Figure 26 for a design image). 3.6mm was chosen based upon solder short issues found with anything closer during the first revision. This resulted in a grid of 14x14 thermoelectric elements for a total of 196 elements.

The 8x8 cm thermoelectric device was constructed but it was not functional. While each of the individual thermoelectric junctions was verified as working with a multimeter, there was not a complete circuit through the device. Due to a combination of imprecision in placing the pellets and variability in their heights, there were air gaps between some pellets and the conductive traces on the PCBs. Attempts were made to sand down the soldered-on pellets to provide a consistent height and to identify the precise location of the issue, but the circuit was not made complete. While it is believed that the issue was air gaps, that is not known with certainty.

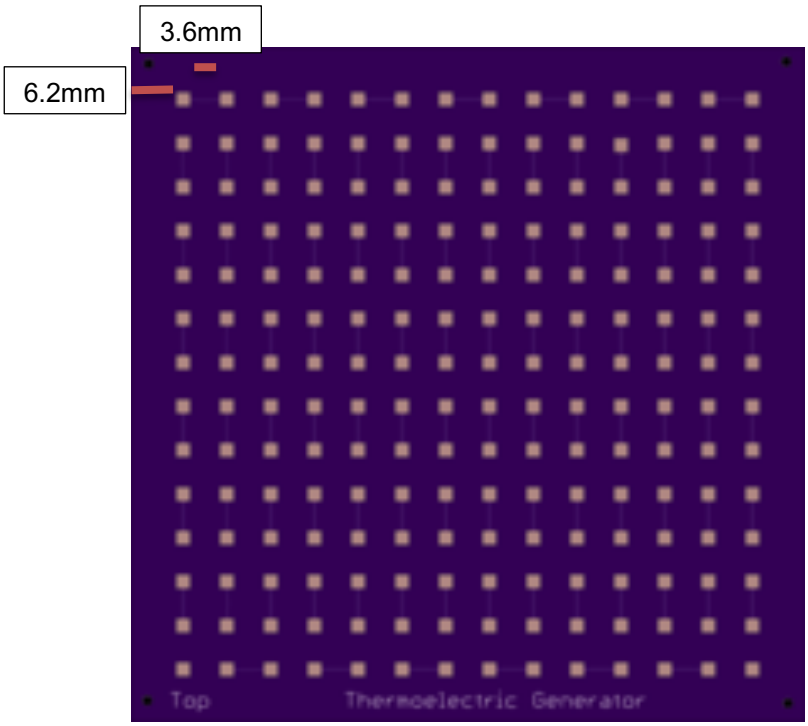


**Figure 26. Revision Two of TEG (8x8cm. 14x14 Thermoelectric Elements)**

As a point of comparison for the number of elements, if the gap between the elements could be reduced by using a machine to 0.1 mm and the buffer could be reduced by 0.2 mm to 6 mm, a grid of 40x40 for a total of 1600 elements would be possible on the same size board. That is over 8 times as many as what the researcher was able to accomplish by hand.[42]

In summary, while the manufacturing approach was validated, the construction of a functional prototype would need to be done with a machine to be able to place as many thermoelectric elements as possible onto the given area and to ensure consistency.

[42] This specific limitation based upon researcher's manual dexterity, others may be able to get a closer grid, but the point remains – without a machine, the spatial efficiency in packing the elements onto the PCB will be limited.

## OVERALL CONCLUSIONS AND FUTURE DIRECTIONS

The original goals of those project were two-fold: (1) to determine whether there was enough thermal energy for a thermoelectric generator (TEG) to be placed onto a LEO small satellite and (2) to design and build a prototype.

On the first point, the combination of on-orbit data analysis and thermal modeling demonstrated that there is an opportunity and it appears to be valuable as specific powers over 100 W/kg were found for modeled TEGs under certain conditions (See Table 8). A TEG can take advantage of energy that solar panels cannot, they are able to produce power even in eclipse unlike a solar panel, and the planar traditional design of TEGs makes the potential integration of them onto the back of a deployed solar panel relatively simple. The next step would be to find a suitable trial mission, characterize the specific opportunity, and place a prototype TEG on it.

On the second part of the project, to design and build a prototype, this project succeeded in part while pointing towards future directions. A PCB sandwich design was validated and has the benefits of being scalable to the room available on the satellite and affords various 2D configurations. However, due to limited tool access resulting in a heavily-manual assembly process being used, a fully-functional prototype wasn’t constructed as a part of this project. For a follow-on, access to a pick-and-place machine would be very helpful if not a necessity.

There are several future directions envisioned. One, due to the

manufacturing issues, comparing the various configuration performance parameters wasn't accomplished but is still believed to be a worthwhile effort for further research. An issue for TEGs is their low efficiencies and testing novel architectures could help alleviate that constraint.

Two, non-planar geometries are an intriguing secondary possibility beyond the back of deployed panels. While the internals of a satellite were shown to have lower temperature gradients than deployed panels, they still have thermal gradients that could be harvested. Additionally, due to the reversible nature of TEGs since they can harvest power from temperature gradients or produce temperature gradients when supplied with power, they are an intriguing component to be used in a thermal control system. A large potential problem is that the space available and thermal flows may not be planar and is likely to vary from satellite to satellite. If TEGs could be tailor-made, it would likely make them easier and more valuable to integrate internally. Traditional manufacturing techniques are often not well-suited to bespoke and geometrically complex shapes. Additive manufacturing presents an option and as research advances on making thermoelectric parts with those processes, there will likely be applications in satellite TEGs.

Three, is to integrate a planar TEG onto the back of a deployed solar panel of a LEO satellite to validate the performance. While modeling and analysis shows a potential opportunity, the real test is to be used in a mission. Due to the relatively unproven nature of this, it is expected and encouraged that the TEG act

as a secondary and non-essential power system to augment solar panels on the test mission. If successful, it may be possible to design missions that rely entirely on TEGs, potentially opening new mission opportunities.

# APPENDIX A: BACKGROUND ON CUBESATS

"Cube Satellite" or "CubeSat" is a form factor that was originally developed in the late 1990's, became popular with researchers, and over the past decade has become increasingly used in the commercial side of the space industry. A CubeSat's body is made up of a set of cubes, each 10 cm per side. CubeSats are generally referred to by the number of cube units, or "U"s, it has. As a frame of reference: a 1U can fit in your hand, a 3U is about the size of a loaf of bread, and a 6U is shoe box-sized. Generally, satellites larger than that stop conforming to the CubeSat standard. For a frame of reference on the size satellites can be, one of the most famous satellites of all time, the Hubble Space Telescope, is about the size of a school bus (Space Telescope Science Institute, n.d.).

To note, there are other terms that often go along with CubeSat or are used almost as synonyms such as 'smallsat' or 'nanosat' although all those terms have different definitions. 'Nanosat', 'microsat', 'smallsat', etc. terms refer to mass while CubeSat refers to a satellite's organizing method. So, a CubeSat could also be a nanosat but isn't always.

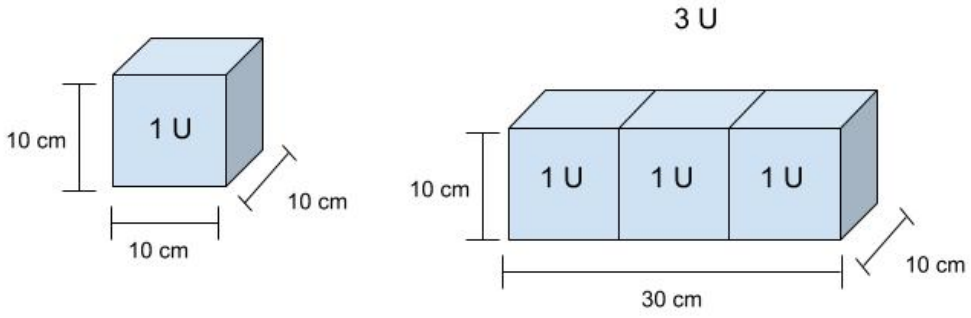


**Figure 27: Diagram of Cube Satellite (CubeSat) Form Factor**

## BIBLIOGRAPHY

List of Abbreviations in Journal Titles

| | |
|---|---|
| AIAA | American Institute of Aeronautics and Astronautics |
| IEEE | Institute of Electrical and Electronics Engineers |
| USU | Utah State University |


Agencia Espacial Civil Ecuatoria. (2016). *DSA: 1U Deployable Solar Arrays.* Retrieved September 18, 2019, from https://www.cubesatshop.com/wp-content/uploads/2016/07/EXA-DSA-Brochure-3C.pdf

Analytical Space, Inc. (2018, February 28). Radix Technical Description. Federal Communications Commission. Retrieved May 7, 2019, from [No static link] Can be found by searching file number 0044-EX-ST-2017 at https://apps.fcc.gov/oetcf/els/reports/GenericSearch.cfm

Analytical Space, Inc. (2019, February 26). Technical Description. Retrieved May 7, 2019, from [No static link] Can be found by searching file number 0306-EX-ST-2019 at https://apps.fcc.gov/oetcf/els/reports/GenericSearch.cfm

Astranis. (n.d.). *MicroGeo: Our first production satellite*. Retrieved November 18, 2019, from Homepage.

Bennett, G., Lombardo, J., Hemler, R., Silverman, G., Whitmore, C., & W.R. Amos, E. (2006). Mission of daring: the general purpose heat source radioisotope thermoelectric generator. *Fourth International Energy Conversion Engineering Conference.* AIAA.

Clark, C., & Kirk, S. (2012, April 24). *Off-the-Shelf, Deployable Solar Panles for CubeSats.* Retrieved September 18, 2019, from http://mstl.atl.calpoly.edu/~workshop/archive/2012/Spring/33-Clark-Solar_Panels.pdf

EnduroSat. (n.d.). *Datasheet: 1U Solar Panel.* Retrieved September 18, 2019, from https://www.endurosat.com/modules-datasheets/Solar%20Panel_1U_Datasheet_Rev1_5.pdf

Halt, T., & Wieger, A. (2019). *Smallsats by the Numbers 2019.* Bryce Space and Technology.

Han, T., & Qiu, C.-W. (2016). Transformation Laplacian metamaterials: recent advances in manipulating thermal and dc fields. *Journal of Optics, 18*(4).

Howell, J. R., Menguc, M. P., & Siegel, R. (2015). *Thermal Radiation Heat Transfer.* CRC Press.

Hunt, L. (1964). The early history of the thermocouple. *Platinum Metals Review, 1*(8), 23-28.

ISI Space. (n.d.). *CubeSat Solar Panels.* Retrieved September 18, 2019, from https://www.isispace.nl/product/isis-cubesat-solar-panels/

Jet Propulsion Laboratory. (n.d.). *Mars Cube One (MarCo)*. Retrieved November 18, 2019, from https://www.jpl.nasa.gov/cubesat/missions/marco.php

Kim, F., Kwon, B., Eom, Y., Lee, J. E., Sangmin Park, S. J., & Park, S. H. (2018). 3D printing of shape-conformable thermoelectric materials using all-inorganic Bi 2 Te 3-based inks. *Nature Energy*, 301.

Laird Thermal Systems, Inc. (n.d.). *387001747.* Retrieved October 25, 2019, from Digi-Key: https://www.digikey.com/product-detail/en/laird-technologies-engineered-thermal-solutions/387001747/1487-1048-ND/8042745

Lappas, V., Tsourdos, A., Kindylides, S., & Kostopoulos, a. V. (2019). A Low Cost Thermoelectric Generator for Small Satellites. *AIAA Scitech 2019 Forum*, 1521.

Longo, C. R., & Rickman, S. L. (1995). *Method for the calculation of spacecraft umbra.* NASA.

Lukowicz, M. V., Abbe, E., Schmiel, T., & Tajmar, M. (2016). Thermoelectric Generators on Satellites—An Approach for Waste Heat Recovery in Space. *Energies, 9*(7), 541.

Lumb, M. P., Mack, S., Schmieder, K. J., González, M., Bennett, M. F., Scheiman, D., & Meitl, M. (2017). GaSb-Based Solar Cells for Full Solar Spectrum Energy Harvesting. *Advanced Energy Materials, 7*(20).

Matthes, C. S., Woerner, D. F., Hendricks, T. J., Fleurial, J. P., Oxnevad, K. I., Barklay, C. D., & Zakrajsek, J. F. (2018). Next-generation radioisotope thermoelectric generator study. *IEEE Aerospace Conference* (pp. 1-9). IEEE.

Nanosats Database. (2019, June 10). *Homepage.* Retrieved October 25, 2019, from Nanosatellite Types: https://www.nanosats.eu/img/fig/Nanosats_types_2019-06-10.pdf

NASA. (2001). *Staying Cool on the ISS*. Retrieved April 15, 2019, from NASA Science: https://science.nasa.gov/science-news/science-at-nasa/2001/ast21mar_1/

NASA. (2017). *Next Generation RTG Study Final Report*. Retrieved March 24, 2019, from https://rps.nasa.gov/resources/73/next-generation-rtg-study-final-report/

NASA. (2019, March 18). *What is a Lagrange Point?* Retrieved May 1, 2019, from https://solarsystem.nasa.gov/resources/754/what-is-a-lagrange-point/

NASA. (n.d.). *Dellingr (RBLE) .* Retrieved November 18, 2019, from Gunter's Space Page: https://space.skyrocket.de/doc_sdat/dellingr.htm

O'Callaghan, J. (2019, October 21). Rocket Lab To Begin Missions To The Moon In 2020 With New 'Photon' Spacecraft. Retrieved November 18, 2019, from https://www-forbes-com.cdn.ampproject.org/c/s/www.forbes.com/sites/jonathanocallaghan/2019/10/21/rocket-lab-to-begin-missions-to-the-moon-with-new-photon-spacecraft/amp/

Oregon State University. (n.d.). *Rebuilding the supply of Pu-238*. Retrieved March 24, 2019, from https://ne.oregonstate.edu/rebuilding-supply-pu-238

Polman, A., Knight, M., Garnett, E. C., Ehrler, B., & Sinke, a. W. (2016). Photovoltaic materials: Present efficiencies and future challenges. *Science, 352*(6283).

Ross, R. T., & Hsiao, T.-L. (1977). Limits on the yield of photochemical solar energy conversion. *Journal of Applied Physics, 48*(11), 4783-4785.

SolAero Technologies. (2016). *ZTJ Space Solar Cell Datasheet.*

Space Telescope Science Institute. (n.d.). *School Bus in the Sky*. Retrieved August 23, 2019, from HubbleSite: http://hubble.stsci.edu/hubble_discoveries/10th/photos/slide01long.shtml

SpaceQuest. (2016). *Product Datasheet SP-C Cubesat Solar Panels.* Retrieved September 18, 2019, from http://www.spacequest.com/shop2/sp-6

Spire. (2015, November 23). Exhibit A - Spire Global, Inc. - Response to Question 43 - FCC Form 312. Retrieved from https://licensing.fcc.gov/myibfs/download.do?attachment_key=1116161

Spire. (n.d.). *Lemur-2.* Retrieved November 18, 2019, from Gunter's Space Page: http://space.skyrocket.de/img_sat/lemur-2__2.jpg

Woerner, D. (2016). A Progress Report on the eMMRTG. *Journal of Electronic Materials, 3*(45), 1278-1283.

Woerner, D. (2017). *Next-Generation Radioisotope Thermoelectric Generator Study Final Report.* NASA Radioisotope Power Subsystem Program, Jet Propulsion Laboratory.

Zimmerman, R., Doan, D., Leung, L., Mason, J., Parsons, N., & Shahid, a. K. (2017). Commissioning the world’s largest satellite constellation. *AIAA/USU Conference Small Satellites. 31.* AIAA.

## CURRICULUM VITAE